



Sijunzi Decoction Targets IL1B and TNF to Reduce Neutrophil Extracellular Traps (NETs) in Ulcerative Colitis: Evidence from Silicon Prediction and Experiment Validation

Dong Zhang ^{1,2}, Siwei Duan³, Zhangyou He⁴, Zeming Zhu³, Zhiping Li³, Qincheng Yi⁴, Tiantian Cai^{1,2}, Juanjuan Li ^{1,2}, Nan Chen^{1,2}, Shaoju Guo^{1,2}

¹Gastrointestinal Ward, The Fourth Clinical Medical College of Guangzhou University of Chinese Medicine, Shenzhen, People's Republic of China; ²Gastrointestinal Ward, Shenzhen Hospital of Traditional Chinese Medicine, Shenzhen, People's Republic of China; ³Institute of Gastroenterology, Science and Technology Innovation Center of Guangzhou University of Chinese Medicine, Guangzhou, People's Republic of China; ⁴Institute of Gastroenterology, Guangzhou University of Chinese Medicine, Guangzhou, People's Republic of China

Correspondence: Shaoju Guo, Gastrointestinal Ward, The Fourth Clinical Medical College of Guangzhou University of Chinese Medicine, Shenzhen, People's Republic of China, Tel +86-0755-82571384, Email gsj1080@163.com

Purpose: This study was conducted to explore the mechanism of Sijunzi Decoction (SJZ) in the treatment of ulcerative colitis (UC).

Methods: The study aimed to investigate the active components and targets of SJZ in the treatment of UC by screening databases such as TCMSP, GeneCards, OMIM, Distinct, TTD, and Drugbank. An online Venn tool, Cytoscape 3.7.2, and Autodock Tools were used to analyze the components and targets. The study also used a mouse model of UC to further investigate the effects of SJZ. HE staining, immunofluorescence, ELISA, qPCR, and Western blot were used to detect various indices.

Results: Eighty-three active components and 112 action targets were identified from SJZ, including 67 targets for treating UC-related NETs. The five core targets identified were AKT1, JUN, IL1B, PTGS2, and TNF, and molecular docking studies indicated that the five targets were well-docked with ginsenoside Rh2, isoflavones, and formononetin. Animal experiments demonstrated that SJZ could alleviate various parameters such as weight, colon length, spleen index, disease activity index, and intestinal pathology of the UC mice. Immunofluorescence and Western blot showed that SJZ could reduce the expression of IL1B and TNF in intestinal neutrophils while increasing the expression of Occludin. Cellular immunofluorescence suggests that SJZ can reduce the expression of TNF and IL1B in NETs. The qPCR results also suggested that SJZ could inhibit TNF signal. Furthermore, ELISA results suggested that SJZ could inhibit the expression of pro-inflammatory cytokines (TNF- α , IL-1 β , IL-6) while promoting the expression of anti-inflammatory cytokines (IL-10, IL-37, TGF- β).

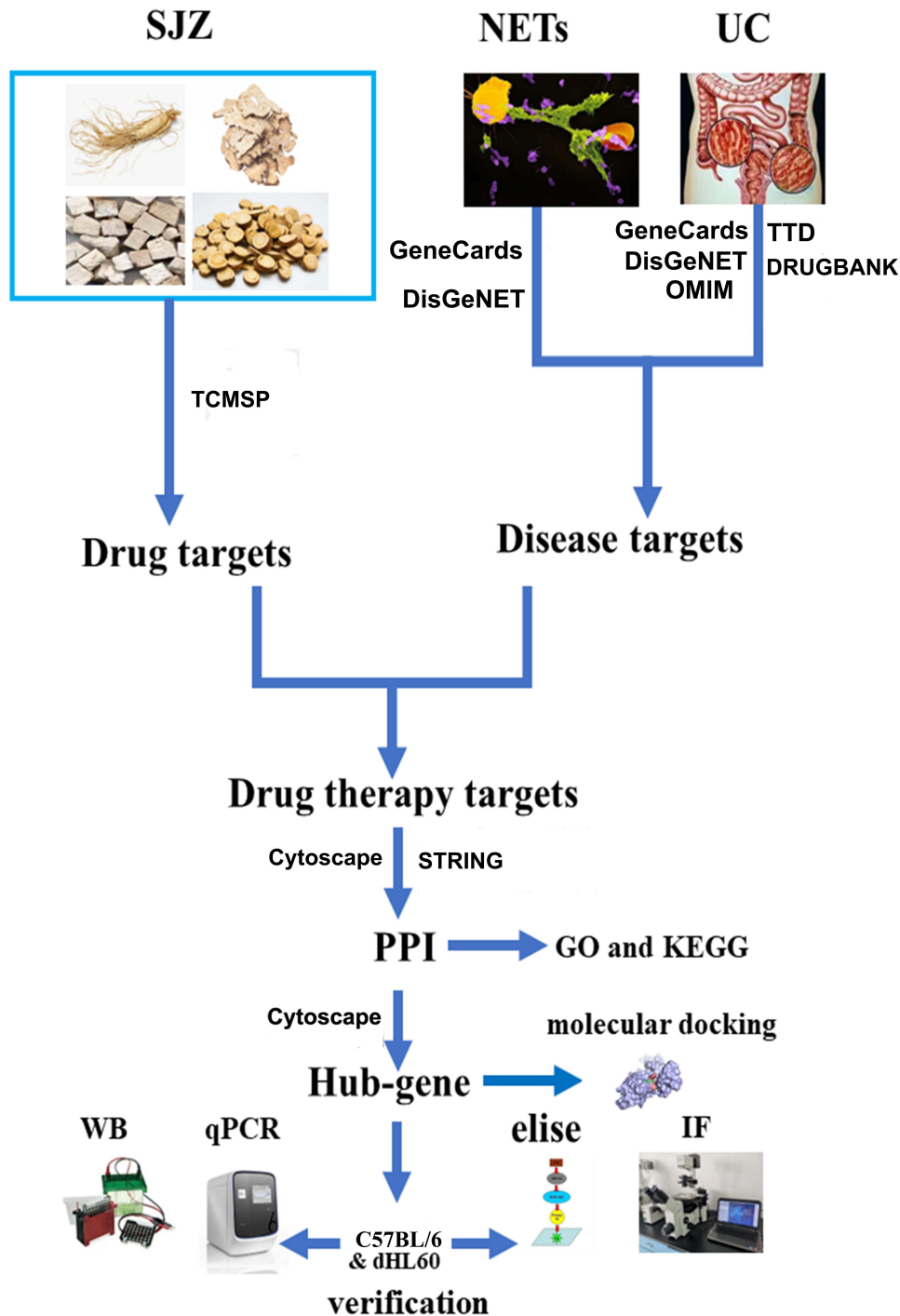
Conclusion: SJZ treats UC by reducing the content of intestinal NETs, with primary targets on the NETs being IL1B and TNF and suppress TNF signal. The practical components of SJZ may be ginsenoside Rh2, isoflavones, and formononetin.

Keywords: ulcerative colitis, Sijunzi decoction, network pharmacology, IL1B, TNF

Introduction

Ulcerative colitis (UC) is a common inflammatory bowel disease characterized by abdominal pain, purulent mucus stool, and intermittent diarrhea.¹ UC has a long course of the disease, recurrent attacks, and cancer-prone characteristics and is currently considered incurable, bringing a severe economic burden to society.² In the past decades, the prevalence of UC has been rising globally.³ A review shows that the incidence of UC in western countries has increased from 0.02% to 0.5%, nearly 25 times.³ The treatment methods of UC mainly include 5-aminosalicylic acid preparations, hormones, immunosuppressants, monoclonal antibody biological agents, and surgery.¹ However, after systematic treatment, 50% of patients still have poor mucosal healing.⁴ Therefore, finding new mechanisms and therapeutic drugs for UC is urgent.

Graphical Abstract



The pathogenesis of UC is complex. The mainstream view is that the etiology of UC is related to intestinal microorganisms, genetic susceptibility, diet and living environment, and imbalance of intestinal mucosal inflammatory immune response, but the specific mechanism has not been resolved.⁵ The imbalance of intestinal mucosal inflammatory

response is the core mechanism of UC.⁵ Many factors cause the imbalance of intestinal mucosal inflammatory response, among which the neutrophil extracellular traps (NETs) is one of the vital pathogenesis.⁶

Neutrophils are a kind of immune cells widely existing in the human body. An essential form of neutrophil driving inflammatory response is achieved through the NETs.⁷ Neutrophils act as the first line of defense against harmful external factors in the intestinal tract.⁸ The early-formed NETs can engulf pathogens to protect the mucosal barrier.⁸ In the later stage, the imbalance of NETs clearance and generation leads to a large number of NETs residues in the intestine, which will cause intestinal mucosal inflammation.⁸ NETs contains many inflammatory factors and proteins that activate many inflammatory signaling pathways.⁹ S100-A9 is also found in NETs as a UC marker.¹⁰ A large number of NETs have been found in the intestinal pathology of patients with clinical UC, and drugs targeting NETs are also conducting relevant clinical experiments.¹¹⁻¹³ To sum up, NETs has been recognized as a promising target for treating UC in the industry.

Traditional Chinese medicine (TCM) offers potential benefits for treating ulcerative colitis (UC) by improving intestinal mucosa healing, reducing recurrences, and enhancing patients' quality of life.¹⁴ While there are no specific studies on TCM's effect on reducing neutrophil extracellular traps (NETs) in UC, research indicates that TCM can reduce NETs levels and alleviate inflammation in lung infections.^{15,16} This indicates that TCM plays a certain role in reducing NETs levels.

TCM identifies spleen deficiency as a fundamental syndrome in UC. Sijunzi decoction (SJZ), known for strengthening the spleen and benefiting qi, has shown remarkable effects in clinical practice.¹⁷ Although the exact mechanism of SJZ in treating UC remains unclear, studies suggest that it can promote mucosal healing, regulate intestinal flora, reduce inflammation, and modulate intestinal immunity.^{18,19} SJZ plays a multifaceted role in UC treatment and contributes to reducing the inflammatory immune response.¹⁹ While NETs are a crucial mechanism in UC inflammation and immune responses, there is limited research on whether SJZ affects NETs. We hypothesize that SJZ may have the potential to treat NETs, opening up a new avenue for investigation.

In this study, network pharmacology identified ginsenoside Rh2, formononetin, and isoflavones in SJZ as potential components for reducing NETs in ulcerative colitis (UC). Further investigations, including molecular docking and animal studies, suggested that SJZ may target TNF and IL1B to reduce NETs and alleviate UC by modulating inflammatory factors. This research on SJZ's molecular mechanisms in UC treatment not only lays a foundation for its broader use but also promotes the modernization of traditional Chinese medicine, facilitating its integration with modern medicine to benefit patients with specific diseases.

Materials and Methods

Collection of Chemical Components and Targets of SJZ

Through the TCMSp platform (<https://old.tcmsp-e.com/tcmsp.php>) for searching the ingredients of Ginseng, *Atractylodes macrocephala*, *Poria cocos*, and Licorice. Set the oral availability (OB) greater than or equal to 30% and drug-like (DL) greater than or equal to 0.18. After the effective ingredients were obtained, search for the active target of a single drug ingredient through its MOLID number. Then use the UniProt (<http://www.uniprot.org>) database to download the compound Excel data table, use the "TRIM" function to optimize the data, and use the "vlookup" function to match the target gene name. The unmatched gene names were supplemented through a literature review. Finally, the relevant target proteins of the chemical components obtained by the above methods will be used by UniProt (<https://www.uniprot.org>) database to annotate it.

Construction of the Compounds-Targets Network

The compounds of SJZ and the targets of SJZ were imported into Cytoscape 3.8.2 software to perform network topology analysis. Adjusted the target figure, color, transparency, and size according to the Degree value (number of gene connections) and construct the "traditional Chinese medicine ingredient target" network diagram. In this study, the "components-targets" network was constructed by using the Cytoscape software (version 3.8.2).

Prediction of Disease Targets

GeneCards (<https://www.genecards.org/>), OMIM (<https://www.omim.org/>), Disgenet (<https://www.disgenet.org/>), TTD (<http://db.idrblab.net/ttd/>) and Durgbank (<https://go.drugbank.com/>) are online network platform and were used to obtain the required disease related pathogenic genes. “Ulcerative colitis” as the keyword to search related targets. Take “neutral extracellular traps” as the key word to search for relevant NETs network targets in GeneCards, Disgenet. Set the object as “human”, use the “VLOOKUP” function to match the target gene name, and screen the intersection genes of drugs and diseases. Venny (<https://bioinfogp.cnb.csic.es/tools/venny/>) software was used to obtain the intersection targets of ulcerative colitis action target and NETs as the potential action target for further research. The mining of the human public database involved was approved by the Ethics Committee of Shenzhen Hospital of Traditional Chinese Medicine. Animal Ethics Committee of Guangzhou University of Chinese Medicine approved animal experiments.

Acquisition of Key Targets

Venny (<http://bioinformatics.psb.ugent.be/webtools/Venn/>) was used to obtain the intersection targetS of the action SJZ’s targets and the UC’s targets related to NETs as potential targets of SJZ’s compounds in treating NETs in UC.

PPI Network Construction and Network Topology Analysis

Through String (<https://string-db.org/>) platform, import intersection genes set the object as homo sapiens, take the highest confidence of 0.900, hide free gene nodes, and obtain protein interaction. The results were imported into the Cytoscape 3.7.2 software, and the network topology parameters were obtained by selecting “network analyzer”. The Degree value is the interconnection between proteins. The gene intersection of the top five degrees were selected as the core targets of SJZ’s compounds in treating NETs in UC.

GO and KEGG Enrichment Analysis

Through Metascape (<http://metascape.org/>), the platform conducts GO (gene ontology) function and KEGG (Kyoto encyclopedia of genes and genomes) pathway enrichment analysis. The intersection targets obtained were imported into the gene list, set the object as “human”, selected personalized research, and set the minimum overlap as 3, the p-value as 0.05, and the minimum concentration as 1.5. After getting the results, make a GO bubble diagram and a KEGG Pathway path diagram. This study used R software to conduct GO and KEGG enrichment analysis on the targets. Import key targets into R software and use cluster profile for enrichment analysis. GO is widely used to annotate the detailed biological process information of genes occurring in the body. KEGG is a signal network structure between biomolecules formed by summarizing and processing a large number of experimental data sets. To analyse the process of the medicinal materials and the setting of $p < 0.05$ is considered statistically significant.

Molecular Docking

By the function analysis of the “network analyzer” in Cytoscape 3.8.2 software, the top five SJZ’s targets with degree value were selected as macromolecular receptors. The structure of small molecules is obtained through PubChem (<https://pubchem.ncbi.nlm.nih.gov/>) database. PDB (<https://www.rcsb.org/>) was used to acquire the core protein macromolecular receptor structure. Import macromolecules and small molecules into AutodockTools 1.5.6 software for docking verification. After water removal and hydrotreating, Pymol is imported for visualization of docking results. The interaction force between ligand and receptor was analyzed by Autodock Vina software, and the 3D conformation of the ligand-receptor was displayed by Pymol software.

Preparation of Tested Drug

Sijunzi Decoction was purchased from Xingyuanchun Pharmacy in Guangzhou and was identified by Chinese medicine professionals as meeting the experimental requirements. The specific information on the composition herbs of Sijunzi Decoction are shown in Table 1. Soak the 230g SJZ for 3h in a ratio of 1:10 of distilled water to the SJZ. After boiling, concentrate to 1000mL. After freeze-drying, prepare the freeze-drying powder into 1g/mL solution with distilled water, filter and sterilize it at -20°C for storage. Finally, we obtained 41.4 g of SJZ freeze-dried powder, with a yield rate of

Table 1 The Information of Herbs in Sijunzi Decoction

Chinese Pinyin Name	Academic Name	Place of Origin	Part of Medicine	Weight (g)	Batch Number
Renshen	<i>Panax ginseng</i> C.A.Mey.	Jilin, China	Root	15g	2,204,573
Baizhu	<i>Atractylodes macrocephala</i> Koidz.	Zhejiang, China	Root	10g	2,107,864
Fuling	<i>Wolfiporia cocos</i> (F.A. Wolf) Ryvarden & Gilb.	Yunnan, China	Root	15g	2,206,187
Gancao	<i>Glycyrrhiza uralensis</i> Fisch. ex DC.	Nei Monggol, China	Root	6g	2,109,386

18%. Mesalazine was purchased from Shanghai Aidifa Pharmaceutical Co., Ltd. (National Drug Approval No. H20143164).

Reagents and Instruments

Dextran sodium sulfate (MP Biomedicals, LOT#S5036). TNF antibody (Abcam, Cat No. ab13847), IL1B antibody (Abcam, Cat No. ab8245), Occludin antibody (Proteintech, Cat No. 27260-1-AP), NE antibody (Abcam, Cat No. ab131260), DAPI (Solarbio, Cat No. C0065), Goat anti-rabbit IgG H&L (Abcam, Cat No. ab150077). Fecal occult blood (OB) reagent (Zhuhai Beso Biotechnology Co., CAS# BA-2020E), Fluorescent microscope (OLYMPUS).

Animal Experiment

Eight-week-old male C57BL/6 were purchased from Zhuhai Bestone Biotechnology Co., Ltd. (production license No. SYXK (Yue) 2020–0229), a total 66. They were randomly divided into the normal group (10 mice), model group (14 mice), SJZ 400 mg/kg group (14 mice), SJZ 800 mg/kg group (14 mice), and 300 mg/kg mesalazine group (14 mice) according to their weight. The normal group drank pure water, and the other groups drank 3% DSS. The control and model groups received 0.2mL saline via gavage, while the drug groups received 0.2mL therapeutic drug via gavage. During this period, the body weight, blood in stool and fecal characteristics of mice were recorded. On the 7th day, the colon length and spleen mass were measured. Disease Activity Index (DAI) = (body mass index+stool shape+blood in stool)/3,²⁰ details are shown in Table 2. Spleen index: spleen mass/body mass. All animal trials were implemented in accordance with the NIH Guide for the Care and Use of Laboratory Animals. Animal Ethics Committee of Guangzhou University of Chinese Medicine approved animal experiments (ethic number #20210903008).

HE Staining

The colon was removed 1.5 cm from the anus, and HE staining was performed after fixation with tissue fixative, ethanol gradient dehydration, xylene transparency, paraffin embedding, and tissue sectioning. Photographs were taken using a fluorescent microscope. The intestinal pathological scoring criteria are used to score the intestinal pathology damage in each group.²¹

Immunofluorescence

The expression of target protein in NETs was determined by double immunofluorescence staining of intestinal tissue. The sections were dewaxed, repaired, incubated, and sealed. Neutrophil-specific antibody NE (Neutrophil Elastase) and IL1B antibody (TNF antibody) were mixed and diluted in equal proportion. The hybrid antibody was added to the sample for

Table 2 DAI Scoring Criteria

Scoring Item	Stool Consistency Score	Rectal Bleeding Score	Body Weight Loss Score
0 points	Normal	No blood	No weight loss
1 point	Soft or slightly loose	Trace blood	Mild weight loss (0–5%)
2 points	Loose or mucous	Moderate blood	Moderate weight loss (5–10%)
3 points	Very loose or watery	Large amount of blood	Significant weight loss (10–15%)

overnight incubation and incubated with two secondary antibodies corresponding to the antibody at room temperature. DAPI was used to dye DNA. After incubation, an anti-fluorescence quenching agent shall be added for sealing. The sections were photographed under a fluorescence microscope. NE, IL1B antibody (TNF antibody), and DNA were co-located and photographed. The intensity of fluorescence value indirectly reflected the expression of IL1B (TNF) in tissue NETs. The content of the Occludin protein was determined by single immunofluorescence staining. The immunofluorescence in each group was analyzed for fluorescence density using ImageJ software.

Western Blot Assay of IL-1B, TNF, and Occludin Expression

The colonic mucosae of the mice were removed and RIPA lysate homogenate containing 1% PMSF was added before centrifuging at 4°C and 13,000 rpm for 15 minutes. The protein concentration of the supernatant was determined by the BCA protein quantitative method. A portion of these samples was mixed with SDS sample buffer and RIPA to solubilize the sample. The 100 µg protein from each sample was loaded onto 5 gels. Then protein was transferred to a PVDF membrane where it was sealed with 5% skimmed milk powder for 1 hour. Added to this and left overnight were the primary antibodies IL1B (1:1000, Abcam), JUN (1:1000, Abcam), occludin (1:1000, Abcam) rabbit antibody, GAPDH rabbit antibody (1:1000, Abcam). After washing, secondary antibodies were added (1:5000), and the sample was incubated at room temperature for 1h prior to ECL. Image Lab software was used to calculate the gray value of the protein bands, and GAPDH was used as a reference for semi-quantitative analysis.

Detection of mRNA Expression in Colon Mucosa by qPCR

To conduct the qPCR analysis the colon mucosae of the mice were ground into homogenate, and the RNA was extracted with TRIzol (Invitrogen). The PrimeScript™ RT reagent Kit with gDNA Eraser (Takara) was used to reverse transcribe it into cDNA. The reaction conditions were: 25°C for 5min, 42°C for 60min, 70°C for 5s, and 4°C for holding. TB Green Premium Ex Taq II (Takara) and cDNA were qPCR reacted, and the reaction system was 20 µ 50 under reaction conditions of: pre denaturation at 95°C for 30s, denaturation at 95°C for 5s, and annealing at 60°C for 30s, for 40 cycles in total. Using GAPDH as an internal reference gene. Relative expression of mRNA of SELE, ICAM1, VCAM1, IL1B, JUN, TNF, PTGS2, AKT1, and NFκ B were determined by the $2^{-\Delta\Delta ct}$ method. Primers were designed and synthesized by Guangzhou Ruizhen Biology. The details of gene sequence can be seen in Table 3.

Table 3 Primer Sequence of TNF Signal Pathway

GENE	Primer	Primer Sequence (5' to 3')
Sele	Sele-F	ATGCCTCGCGCTTTCTCTC
Sele	Sele-R	GTAGTCCCCTGACAGTATGC
ICAM1	ICAM1-F	GTGATGCTCAGGTATCCATCCA
ICAM1	ICAM1-R	CACAGTTCTCAAAGCACAGCG
Vcam1	Vcam1-F	AGTTGGGGATTTCGGTTGTTCT
Vcam1	Vcam1-R	CCCCTCATTCTTACCACCC
JUN	JUN-F	CCTTCTACGACGATGCCCTC
JUN	JUN-R	GGTTCAAGGTCATGCTCTGTTT
TNF	TNF-F	CCCTCACACTCAGATCATCTTCT
TNF	TNF-R	GCTACGACGTGGGCTACAG
PTGS2	PTGS2-F	TTCAACACACTCTATCACTGGC
PTGS2	PTGS2-R	AGAAGCGTTTGCGGTACTION
Akt1	Akt1-F	ATGAACGACGTAGCCATTGTG
Akt1	Akt1-R	TTGTAGCCAATAAAGGTGCCAT
Nfkb	Nfkb-F	ATGGCAGACGATGATCCCTAC
Nfkb	Nfkb-R	TGTTGACAGTGGTATTTCTGGTG

Detection of Serum Inflammatory Factors by ELISA

The peripheral blood serum of the mice was removed, and the supernatant was taken after standing at room temperature for 30 min, being centrifuged at 4°C and 3000 rpm for 15 min. The steps for executing the ELISA kit testing (Jiangsu MEIMIAN) were as follows. The samples and standards were prepared enzyme labeled reagents were added and incubated at 37°C to react, the plates were washed 5 times, color reagents A and B were added at 37°C for 10 minutes, termination solution was added, and readings were taken with the enzyme-labeled instrument. The detected indices were: TNF- α , IL-6, IL-1 β , IL-33, IL-10, and TGF- β .

Determination of Components in SJZ by LC-MS

Weigh 0.15 g of SJZ freeze-dried powder, add 1000 μ L 80% methanols and grinding beads, grind up 5 mins, and then vortex for 10 mins. Centrifuge at 4 °C for 10 mins with a centrifugal force of 20,000 \times g. Take the supernatant and filter it for analysis. Use UltiMate 3000 RS for analysis and detection. The detection conditions are as follows: chromatographic column: AQ-C18, 150 \times 2.1mm, 1.8 μ m, Welch; flow rate: 0.30 mL/min; Water phase: 0.1% formic acid/water solution; Organic phase: methanol; Column temperature box temperature: 35 °C; Automatic sampler temperature: 10.0 °C; Sample volume of automatic sampler: 5.00 μ L. The data collected from the high resolution liquid quality were preliminarily collated by CD2.1 (Thermo Fisher) and then compared with the database (mzCloud).

Culture of dHL-60 and Construction of NETs Model

Human promyelocytic leukemia cell (HL-60) was purchased from the cell bank of the Chinese Academy of Sciences. HL-60 was cultured at 37°C in a 5% CO₂ incubator with IMDM containing 20% fetal serum and 1% penicillin-streptomycin liquid. DMSO (Sigma, No. 67–68-5) was added to HL-60 cell culture at a final concentration of 1.5% (V/V) to induce HL-60 to become neutrophil-like dHL-60 for 7 days, with fluid changes every other day. dHL-60 was counted and inoculated in 24-well plates. Phorbol myristate acetate (PMA) was added to the cell culture wells to a final concentration of 50 nM and stimulated for 4 h to produce NETs.

Preparation of SJZ Medicated Serum (SJMS)

The lyophilized powder of SJZ was converted into a dose of 400 mg/kg (medium dose) for mice according to the actual human dose. We gavaged mice with 800mg/kg (high dose) twice a day for 3 days. After the last gavage, the mice were sacrificed and peripheral blood was taken. The peripheral blood was centrifuged at 3000rpm, 4°C for 15min, and the serum was stored at –80°C. The high-dose SJMS was diluted into medium SJZMS with PBS at a ratio of 1/2 before use. DHL-60 was molded in NETs, and the cells were divided into normal group, model group, medium-dose SJMS group, high-dose SJMS group, and mesalazine 40 mM group.^{22,23}

Cellular Immunofluorescence

Cells to be tested were fixed with 4% paraformaldehyde for 20 min at room temperature; washed 3 times with PBS for 5 min each; permeabilized with 0.3% Triton X-100 for 10 min; washed 3 times with PBS for 5 min each; blocked with 2% BSA for 1 h, washed 3 times with PBS for 5 min each; cells were incubated with antibody and incubated overnight at 4°C in a wet box; washed 3 times with PBS for 5 min each. The cells were incubated with antibodies overnight at 4°C in a wet cassette; washed 3 times with PBS for 5 min; incubated with fluorescent secondary antibody for 30 min at room temperature; washed 3 times with PBS for 5 min; added DAPI for DNA staining for 15 min; washed 3 times with PBS for 5 min; and sealed with anti-fluorescent quenching agent. Photographs were quickly recorded under a fluorescent microscope.

Statistical Analysis

SPSS21.0 was used for all statistical analysis of our experimental data, and GraphPad Prism 7.0 was applied to plot data statistics. The recorded data were expressed as mean \pm standard deviation, and the inter-group comparison of measurement data subject to normal distribution was done using either *t*-test or analysis of variance (ANOVA). If the experimental data obtained were not normally distributed, we used the nonparametric rank sum test instead, and for

count-type data, we used a chi-squared test. $P < 0.05$ was considered to indicate statistically significant test results for all tests.

Results

Active Components and Target of SJZ

Using $OB \geq 30\%$ and $DL \geq 0.18$ as screening conditions in the TCMSP database, 83 active ingredients were obtained after removing duplicates, including 17 ginseng, 6 poria, 4 *Atractylodes macrocephala* and 56 licorice (Figure 1B and Supplementary Table 1). After the duplications were removed, the remaining ingredients corresponded to 112 targets that were used to construct a component-target network (Figure 1B and Supplementary Table 2). From this figure we can clearly see that a great deal of components of SJZ decoction act on different targets, and different components also act on the same target (Figure 1B), which is consistent with the characteristics of SJZ as described by TCM. Licorice corresponded to the most targets of SJZ, followed by ginseng.

Screening of NETs-Related Targets in UC

Through searching the GeneCards, OMIM, TTD, and DrugBank databases, 3199 UC-related targets were obtained (Figure 1A and Supplementary Table 3), and 6576 NETs-related target genes were found by searching the GeneCards, DrugBank, and Disgene databases (Figure 1A and Supplementary Table 4). Finally, after taking the intersection of the two data sets, we were left with 1733 NETs-related targets in UC (Figure 1A). Importantly, NETs-related targets accounted for 55% of UC pathogenic targets, indicating that NETs are crucial to the development of UC.

Screening of Therapeutic Targets of SJZ for NETs in UC

The intersection of the NETs-related targets in UC and the SJZ targets resulted in 67 action targets (Figure 1C). These 67 targets account for 59.8% of all therapeutic targets of SJZ, indicating that NETs may be one of the most important targets of SJZ in treating UC.

PPI Network Construction for Therapeutic Targets of SJZ

Using String and Cytoscape 3.7.2 software, we successfully built a PPI (protein-protein interaction) network of NETs targets, including the above 67 targets, and 671 lines (Figure 1D). The first five core gene targets were AKT1, JUN, IL1B, PTGS2, and TNF based on degree. These five genes and the core indicators ELANE and PADI4 of NETs were introduced into the string for network analysis (Figure 1E), and this revealed that TNF and IL1B genes were associated with ELANE and PADI4. Thus, we selected TNF and IL1B as validation indicators in our subsequent animal experiments.

GO and KEGG Enrichment Analysis of Therapeutic Targets of SJZ

The Molecular Function and Cellular Component of therapeutic targets of SJZ mainly focused on nuclear receptor activity, ligand-activated transcription factor activity membrane raft, membrane microdomain, membrane region (Figure 2A and B). The enrichment and analysis of Biological Process mainly focused on inflammation and immunity, such as the response to lipopolysaccharides and molecules of bacterial origin (Figure 2C). By contrast, the enrichment and analysis of the KEGG pathway mainly focused on inflammation pathways such as the TNF signaling pathway and the IL-17 signaling pathway (Figure 2D). We selected TNF signal to validate the pharmacodynamic effect of SJZ on UC.

Compound Target Core Protein Molecular Docking Validation

Molecular docking binding heat $< -1 \text{ kcal} \cdot \text{mol}^{-1}$ indicates critical activity and $< -5 \text{ kcal} \cdot \text{mol}^{-1}$ shows good binding activity. We observed that Ginsenoside Rh2, isoflavones, and emodin had good binding activity with the five core protein receptors mentioned above (Figure 3, Figure 4 and Table 4). We also confirmed that these compounds were all in SJZ by LC-MS (Supplementary Table 5).

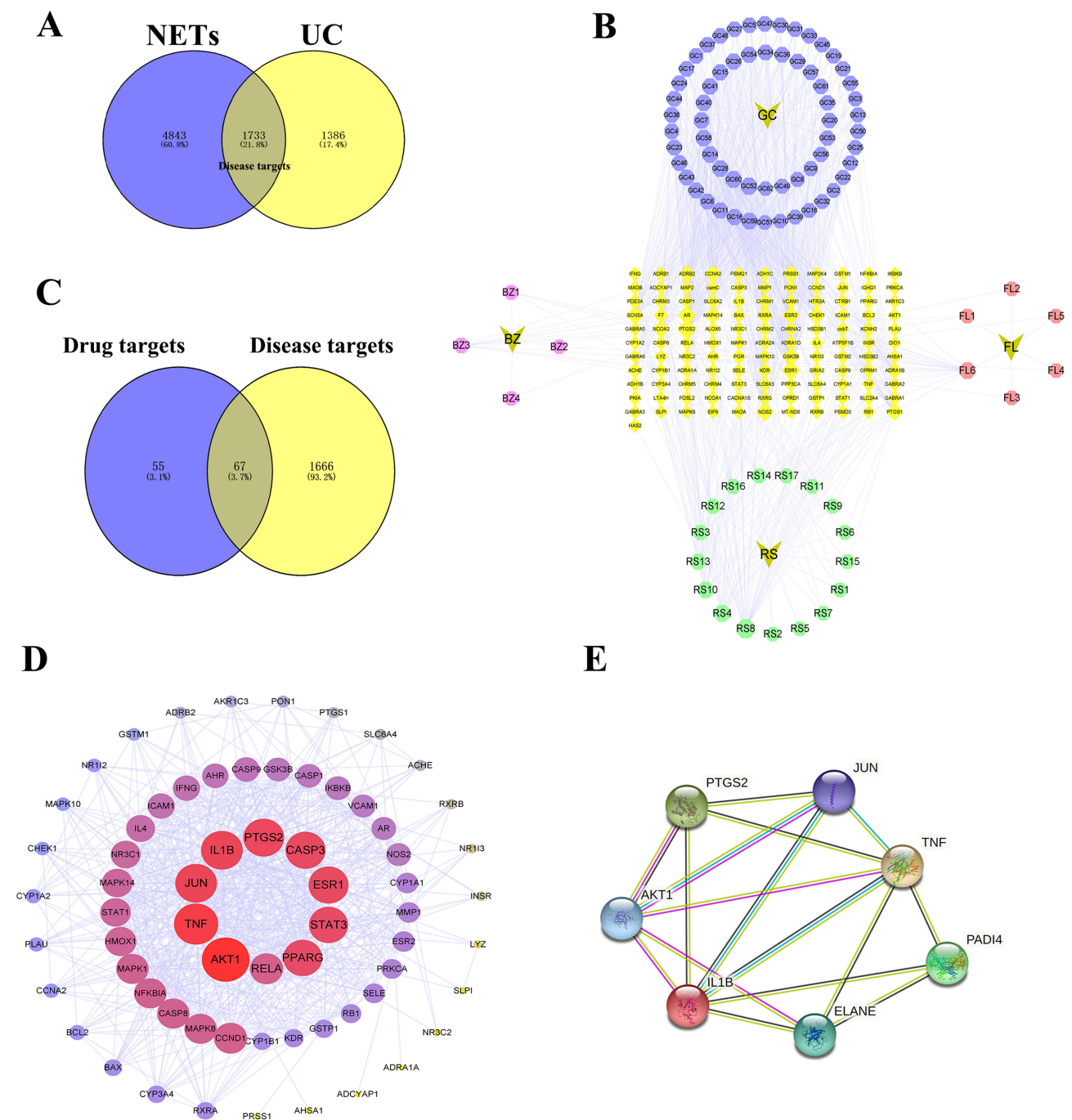


Figure 1 Network pharmacological analysis of SJZ (A) Venn diagram of NETs targets and UC pathogenic targets; (B) Components-target network of SJZ; (C) Venn diagram of action targets (drug targets) of SJZ and related targets (disease targets) of NETs in UC; (D) PPI network of NETs related targets in the treatment of UC with Sijunzi decoction; (E) The network map of the core genes (AKT1, IL1B, PTGS2, JUN, TNF) and the core genes (ELANE, PADI4) of NETs for the treatment of SJZ.

Animal Model Validation

The results of our animal experiments showed that the bodyweight of the model and medication groups decreased significantly after the third day. Furthermore, from the third to the seventh day, the weight of the model group was remarkably reduced compared to the normal group ($P < 0.01$), indicating that the modeling was successful (Figure 5A). Weight loss in the medication group was significantly lower than in the model group as well ($P < 0.01$) (Figure 5A). DAI is an extremely important index for evaluating colitis in mice, and in our experiments the DAI in the model group was strikingly higher than in the normal group from the third day on ($P < 0.01$) (Figure 5B). In comparison, the DAI in the

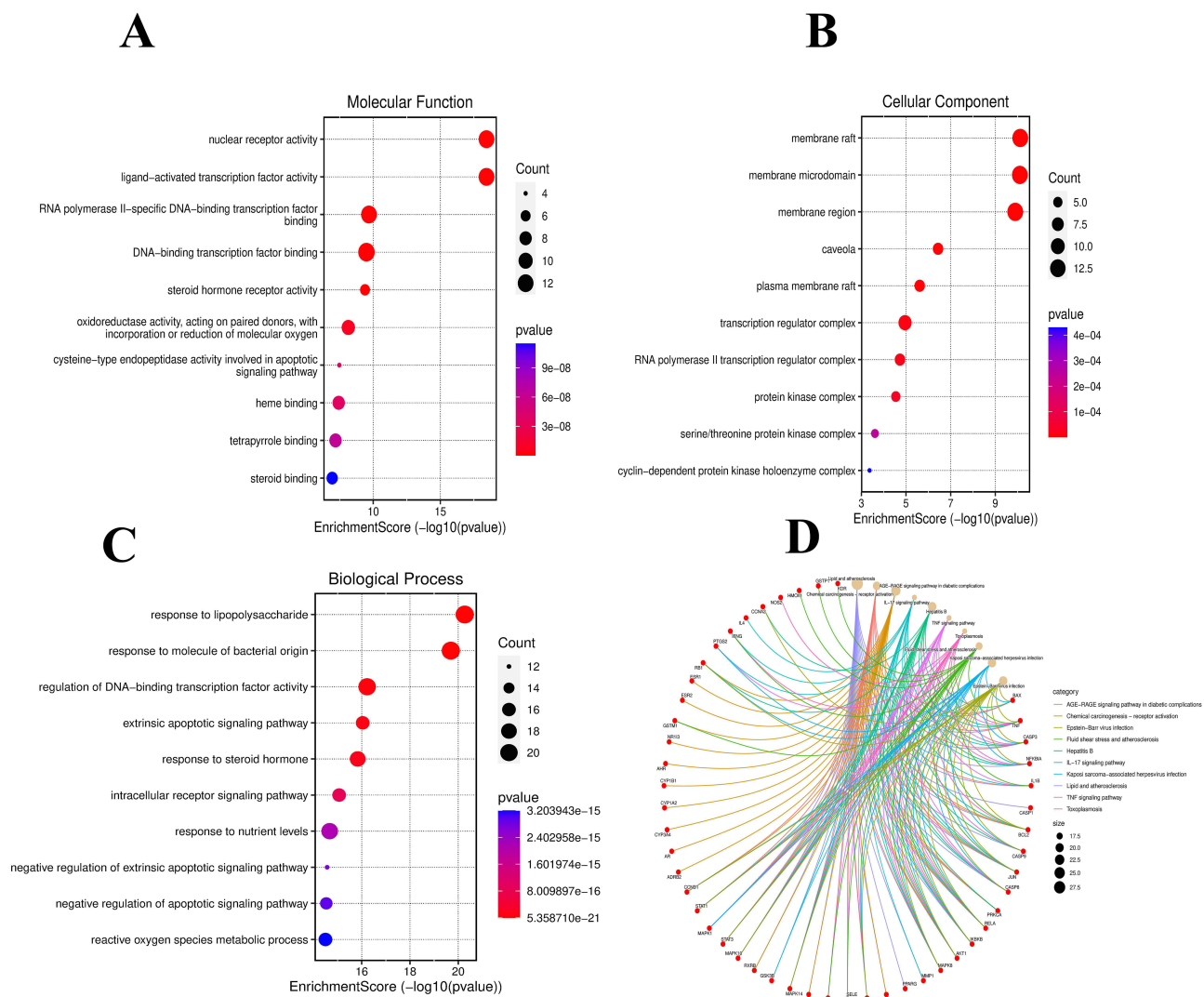


Figure 2 GO and KEGG analysis of NETs-related targets in SJZ treatment of UC. (A) Molecular function analysis; (B) Cellular component analysis; (C) Biological process analysis; (D) KEGG pathway analysis.

drug group was significantly lower compared to the model group ($P < 0.01$) (Figure 5B). The intestinal pathology scoring criteria are detailed in Table 5.

In the inflammatory model mice, the colon length was inversely proportional to the inflammatory reaction, and the spleen index was proportional to the degree of the inflammatory reaction. Moreover, the colon length of the DSS modeling group was significantly lower than the blank control group without any treatment ($P < 0.01$) (Figure 5C and D), and the spleen index was markedly higher than the normal group ($P < 0.05$) (Figure 5E and F). Compared to the model group, the colon length in the mice treated with drugs was significantly longer than the model mice treated with DSS as well ($P < 0.01$) (Figure 5C and D), and this group's spleen index was also remarkably lower than the model group's spleen index ($P < 0.05$) (Figure 5E and F). Our intestinal pathological examinations also found that the intestinal structural integrity of the model group was damaged, the mucosa was swollen, and the villi were shortened. The drug group maintained its normal structure, however, with a small amount of villus defects and a slight swelling of the mucosa (Figure 6A and C). The above evidence shows that SJZ had an effect on the treatment of enteritis in the mice. There was no statistically significant difference observed when comparing 400mg/kg SJZ and 800mg/kg SJZ with 300mg/kg Mesalazine, indicating that the efficacy of these three in treating UC mouse models is similar.

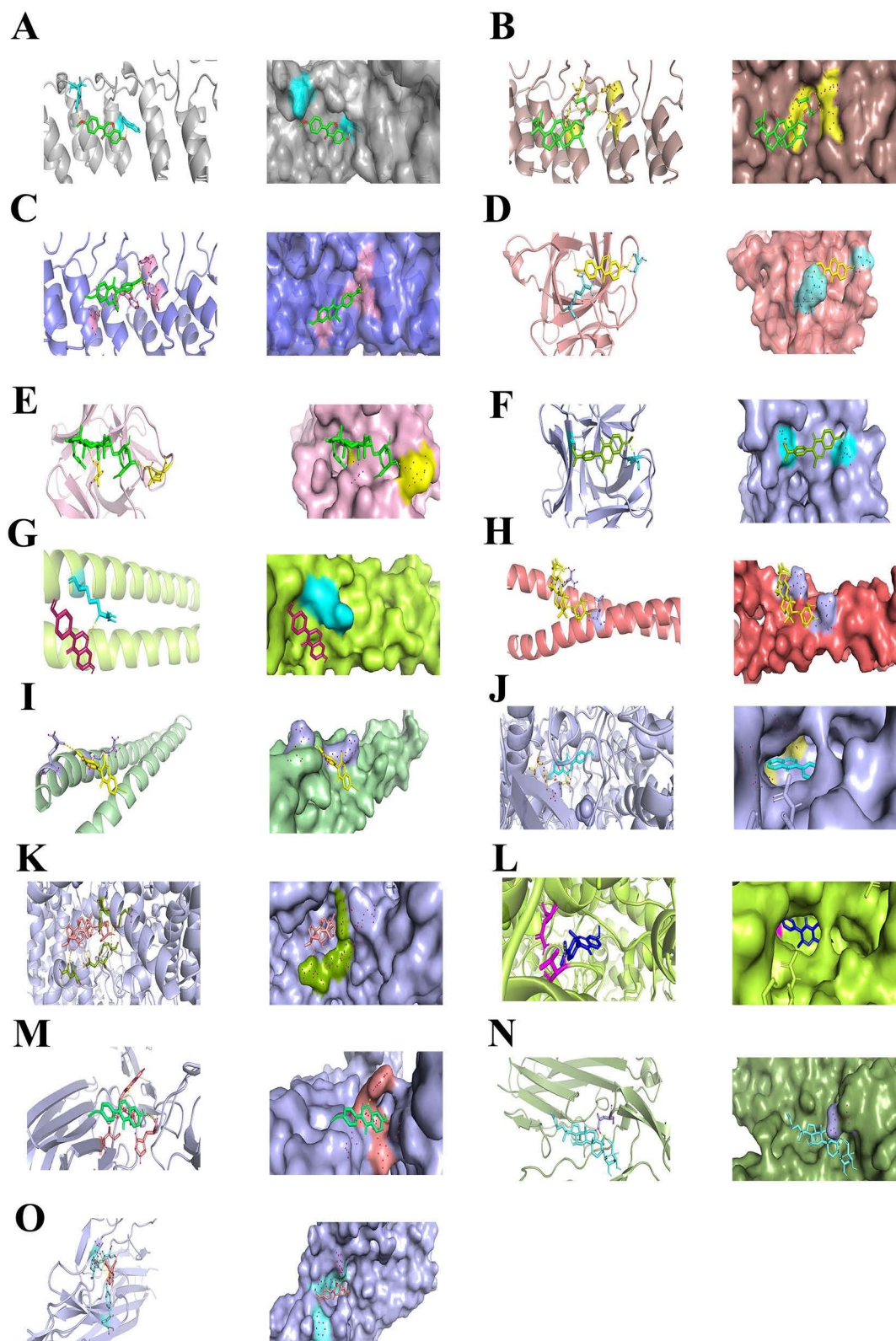


Figure 3 Molecular docking between the core gene of the therapeutic targets of SJZ and the corresponding compounds. **(A)** Molecular docking between AKT1 and formononetin; **(B)** Molecular docking between IL1B and formononetin; **(C)** Molecular docking between IL1B and Ginsenoside Rh2; **(D)** Molecular docking between IL1B and isoflavones; **(E)** Molecular docking between IL1B and Ginsenoside Rh2; **(F)** Molecular docking between IL1B and isoflavones; **(G)** Molecular docking between JUN and formononetin; **(H)** Molecular docking between JUN and Ginsenoside Rh2; **(I)** Molecular docking between JUN and isoflavones; **(J)** Molecular docking between PTGS2 and formononetin; **(K)** Molecular docking between PTGS2 and Ginsenoside Rh2; **(L)** Molecular docking between PTGS2 and isoflavones; **(M)** Molecular docking between TNF and formononetin; **(N)** Molecular docking between TNF and Ginsenoside Rh2; **(O)** Molecular docking between TNF and isoflavones.

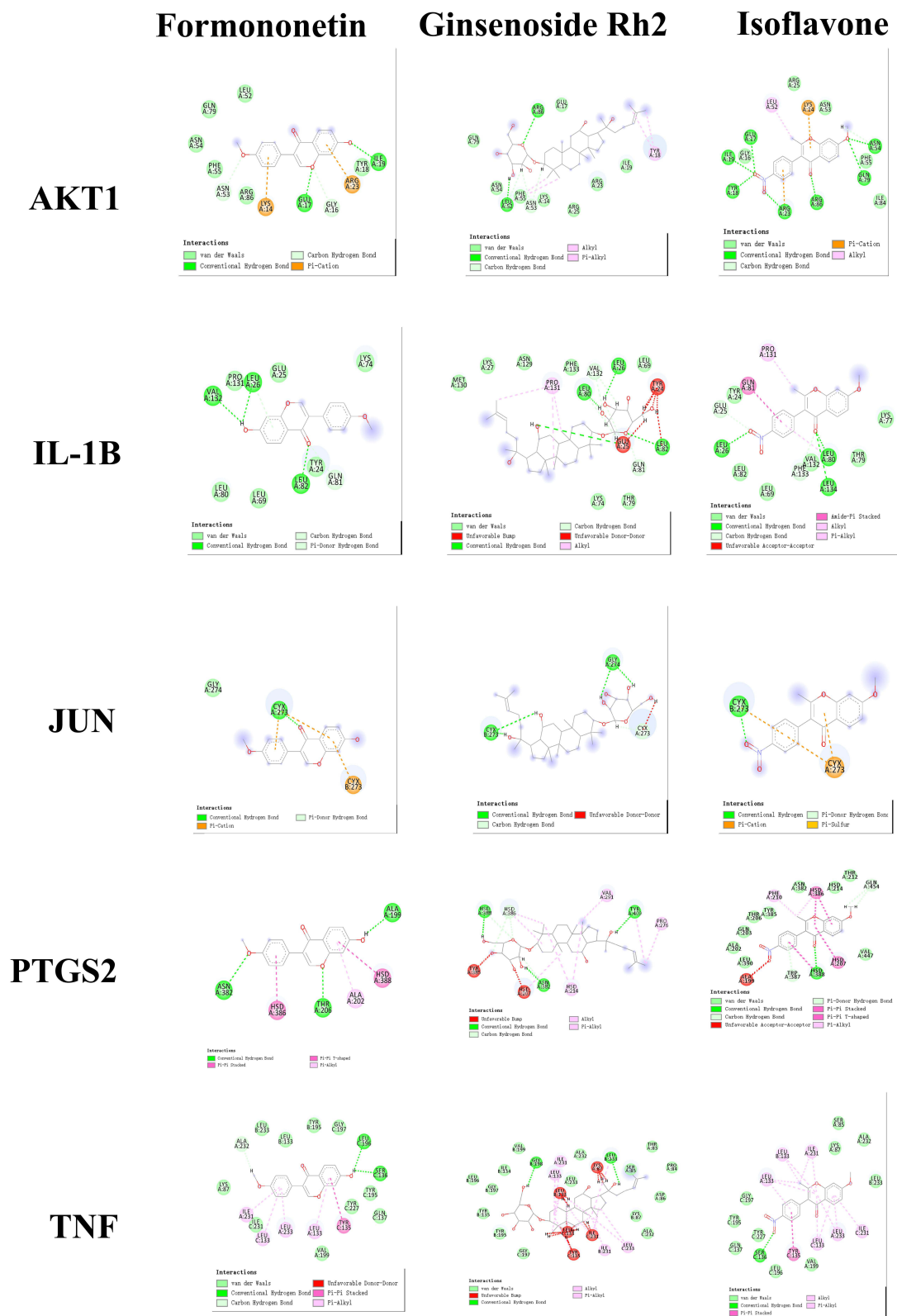


Figure 4 The atomic-amino acid linkage between the core gene of the therapeutic targets of SJZ and the corresponding compounds.

Detection of NETs in UC by Immunofluorescence

We used the double staining method to determine the expression of detection indicators in intestinal neutrophils, which can indirectly reflect the content of NETs. First, NE, a neutrophil marker protein, was co-stained with the target protein

Table 4 Molecular Docking of Core Genes and Corresponding Compounds

kcal.mol ⁻¹	AKT1	TNF	JUN	IL1B	PTGS2
Ginsenoside Rh2	-8.57	-5.8	-5.23	-5.3	-5.68
Formononetin	-6.47	-5.13	-6.7	-4.36	-6.16
Isoflavones	-6.8	-6.18	-6.31	-6.7	-5.32

IL1B (TNF). The intensity of immunofluorescence reflects the content of the detected index, and our results clearly show that the content of IL1B and TNF in neutrophils of the mice in the model group was significantly higher than that of the normal group (Figure 6B and D). However, the content of IL1B and TNF of the mice in the normal group was markedly lower than that of the model group (Figure 7A and B). There was no statistically significant difference observed when comparing 400mg/kg SJZ and 800mg/kg SJZ with 300mg/kg Mesalazine.

Additionally, through the immunofluorescence detection of occludin in the intestinal tissues of each group, we found that the fluorescence value of occludin in the model group was significantly lower than that in the normal group (Figure 8A and B). Still, the fluorescence intensity of occludin protein in the intestinal tissues of mice in the drug treatment group was significantly higher than that in the model group (Figure 8A and B). Thus, SJZ was effective in maintaining the integrity of the intestinal structure. The above evidence shows that the targets of SJZ in treating enteritis mice may be IL1B and TNF. There was no statistically significant difference observed when comparing 400mg/kg SJZ and 800mg/kg SJZ with 300mg/kg Mesalazine.

Western-Blot-Detected TNF, IL1B, and Occludin

The expressions of TNF, IL1B, and occludin proteins in the intestinal mucosa of the mice were detected by Western blot. The Western blot results showed that the contents of TNF and IL1B in the model group were higher than those in the normal group but the occludin was lower (Figure 9). TNF and IL1B in the medication groups (400mg/kg SJZ, SJZ 800mg/kg SJZ, or 300 mg/kg Mesalazine) were lower than those in the model group as well, but occludin was higher (Figure 9). These experimental results suggest that SJZ increased the expression of occludin, a mucosal barrier marker, at the protein level and thus reduced the expression of TNF and IL1B, thereby promoting mucosal healing.

Detection of TNF Signal Indicators by qPCR

TNF signal was screened as the main signal pathway for SJZ (Figure 10) using qPCR analysis the mouse intestinal mucosal tissue. Compared to the normal group, the TNF-signal-related proteins (SELE, ICAM1, VCAM1, IL1B, JUN, TNF, PTGS2, AKT1, and NF κ B) increased in the model group ($P < 0.01$) (Figure 11), but compared to the model group, the TNF-signal-related indicators (SELE, ICAM1, VCAM1, IL1B, JUN, TNF, PTGS2, and AKT1) in the treatment groups (SJZ 400 mg/kg, SJZ 800 mg/kg, or mesalazine 300 mg/kg) were lower than those in the model group ($P < 0.01$) (Figure 11). These results show that SJZ reduced inflammatory mucosal reaction by inhibiting the TNF signal pathway, thus relieving UC. When comparing 400mg/kg SJZ with 300mg/kg Mesalazine, the qPCR levels of proteins PTGS2, SELE, and VCAM1 were significantly lower in 300mg/kg Mesalazine. Additionally, when comparing 400mg/kg SJZ with 800mg/kg SJZ, the qPCR content of SELE was significantly lower in 800mg/kg SJZ. However, there were no statistically significant differences in the qPCR levels of TNF, IL1B, and NF κ B when comparing 400mg/kg SJZ and 800mg/kg SJZ with 300mg/kg Mesalazine.

Detection of Serum Inflammatory Indices in Mice by ELISA

In order to evaluate the therapeutic effects of SJZ even further, we detected pro-inflammatory and anti-inflammatory cytokines in the peripheral serum of the mice. The results suggest that compared to the normal group, the pro-inflammatory factors (IL-1 β , TNF- α , and IL-6) increased in the model group, but the anti-inflammatory factors (IL-10, IL-37, and TGF- β) decreased (Figure 12). Compared to the model group, the treatment groups (SJZ 400 mg/kg, SJZ

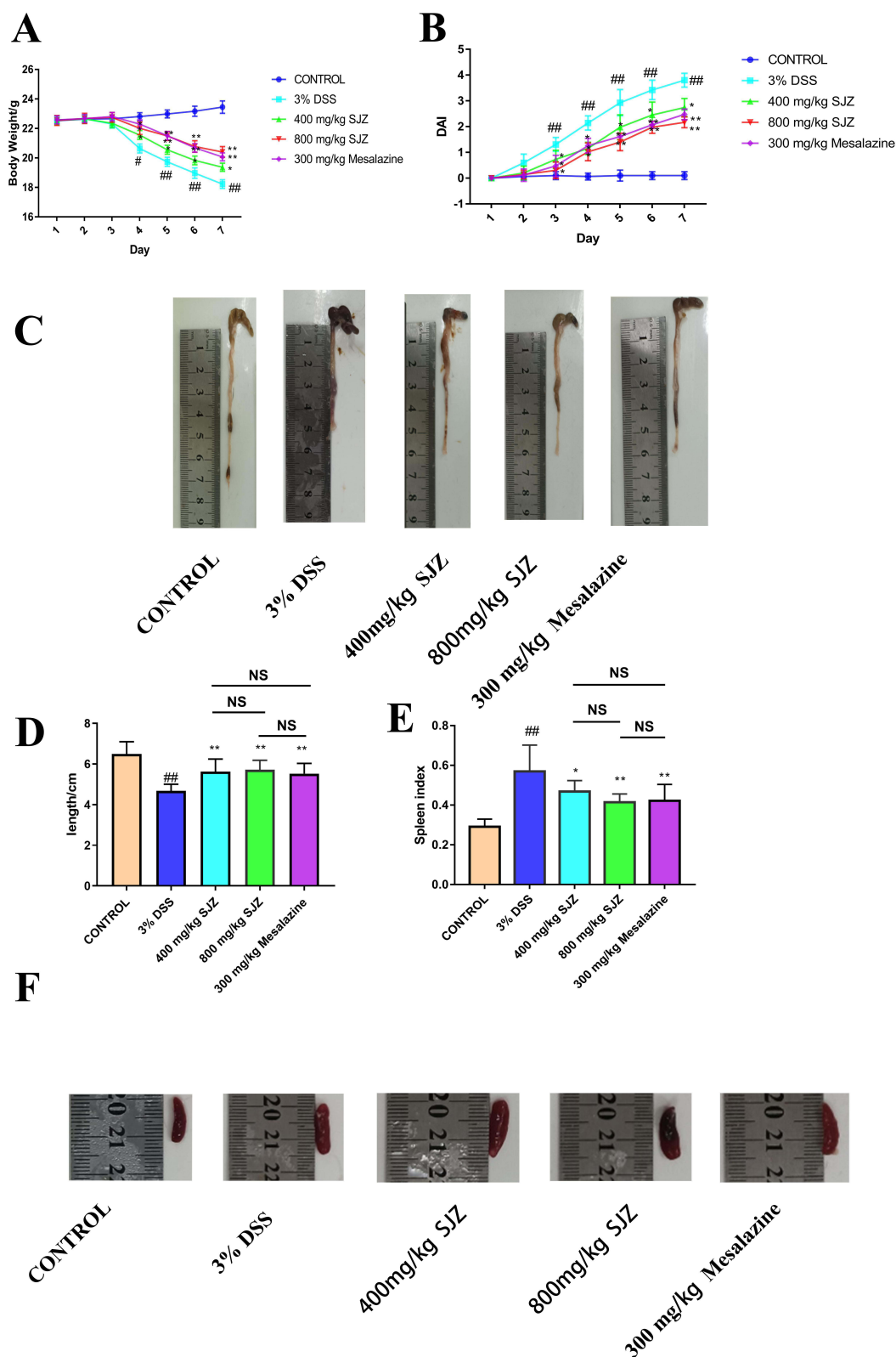


Figure 5 Animal experimental verification of SJZ. (A) Body weight change curve of each group; (B) DAI change curve of each group; (C and D): colon length of each group; (E and F): spleen index of each group. #Compared with the normal group, $P < 0.05$; ##Compared with the normal group, $P < 0.01$; *Compared with the model group, $P < 0.05$; **Compared with the model group, $P < 0.01$; NS: no significance. $n = 10$ (control group), $n = 14$ (model group), $n = 14$ (SJZ 400 mg/kg group), $n = 14$ (SJZ 800 mg/kg group), $n = 14$ (300 mg/kg mesalazine group), each repetition is an independent experiment.

Table 5 Intestinal Pathological Scoring Criteria

Score	Inflammatory Cells Infiltration	Depth of Invasion	Crypt Injury	Pathological Range (%)
0	None	None	None	0
1	±	Mucosa layer	1/3	1–25
2	+	Mucosa and submucosa	2/3	26–50
3	++	Full	Full	51–75
4	+++			76–100

800 mg/kg, or mesalazine 300 mg/kg) had pro-inflammatory factor (IL-1 β , TNF- α , and IL-6) decreases and anti-inflammatory cytokine (IL-10, IL-37, and TGF- β) increases (Figure 12). These results suggest that SJZ can reduce the level of pro-inflammatory factors and increase the level of anti-inflammatory factors. In all of the above-mentioned ELISA assay parameters, there were no statistically significant differences observed when comparing 400mg/kg SJZ and 800mg/kg SJZ with 300mg/kg Mesalazine.

Immunofluorescence Detection of TNF and IL1B in a Cellular Model of NETs

At the cellular level we constructed NETs models by PMA induction of dHL-60. The expression of IL1B and TNF in NETs was detected by immunofluorescence. Compared with the control group, the expression of TNF and IL1B was higher in the model group (Figure 13A and B); compared with the model group, the expression of TNF and IL1B was lower in the drug group (Figure 14A and B). The results of cellular experiments showed that SJZ could reduce the expression of TNF and IL1B in NETs. In the immunofluorescence detection of TNF and IL1B, there were no statistically significant differences observed when comparing 400mg/kg SJZ and 800mg/kg SJZ with 300mg/kg Mesalazine.

Discussion

TCM compounds have a significant effect in treating diseases in clinical applications, but the unclear therapeutic mechanism hinders its further application. Network pharmacology is a more efficient strategy for screening the therapeutic agent of TCM.²⁴ By using the network pharmacology method, we can predict TCM's targets and signal pathways in treating diseases and uncover the main components and therapeutic targets that have therapeutic effects. Ulcerative colitis is a kind of chronic inflammatory bowel. The prevalence of ulcerative colitis in young and middle-aged people is high.² UC is easy to recur, difficult to cure, liable to cancer.² UC seriously impacts the patient's quality of life and a serious burden on the social economy.³ TCM has advantages in the treatment of ulcerative colitis: improving mucosal healing, reducing recurrence, and improving the patient's quality of life.²⁵ Sijunzi decoction, the representative prescription for Invigorating Spleen and Qi in TCM, has gained an excellent effect in the clinical treatment of ulcerative colitis,¹⁷ and the specific mechanism has not been clarified. In terms of efficacy and detection indicators, there were no statistically significant differences between 400mg/kg SJZ and 800mg/kg SJZ compared to 300mg/kg Mesalazine (Figure 5D and E) (Figure 6C and D) (Figure 7A and B). These results suggest that SJZ and Mesalazine have similar effects in treating UC. Considering that the components of SJZ are all derived from medicinal and food ingredients, using SJZ for UC treatment can also avoid the potential long-term side effects associated with Mesalazine treatment, such as upper gastrointestinal bleeding and liver and kidney function impairment.

NETs is one of the important elements causing UC.⁸ In this research, we screened out the pathogenic targets containing NETs in UC and selected 64 targets of SJZ acting on NETs in UC. Five important targets, AKT1, PTGS2, JUN, IL1B, and TNF (Figure 1E), were identified in 64 bits through the topological structure of Degree. These five genes are well-docked with the corresponding compounds: ginsenoside Rh2, isoflavones, and anthoxanthin (Figures 3 and 4). In the UC mouse model, we have determined that SJZ can reduce the intestinal inflammatory response of colitis mice and maintain the integrity of the intestinal mucosal barrier structure (Figures 5 and 9). The mechanism of SJZ in treating

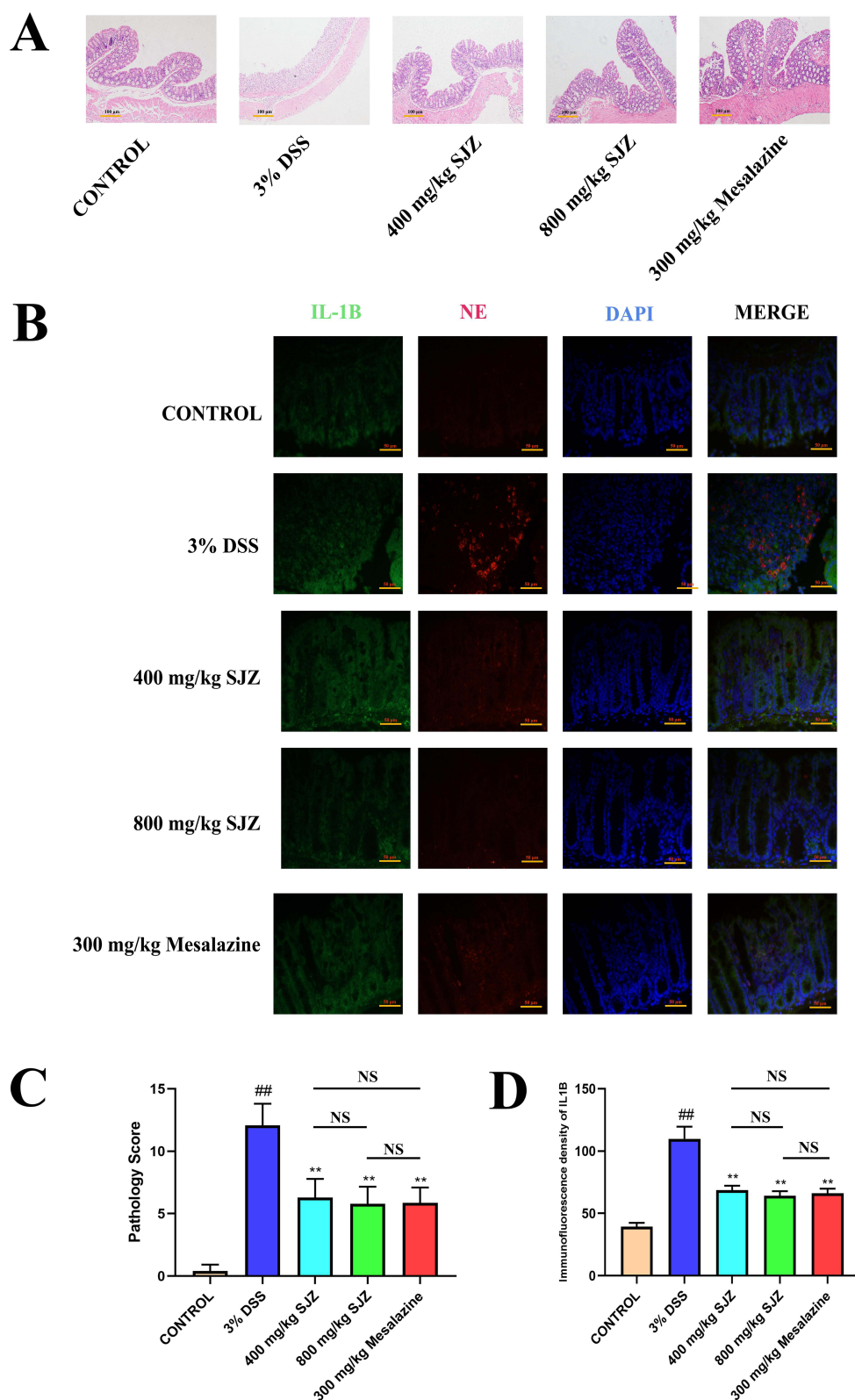


Figure 6 Colon pathology and intestinal immunofluorescence double staining in each experimental animal group. **(A)** Pathology of the colon in each animal experiment group; **(B)** Colon IL1B and NE immunofluorescence double staining was performed in each animal experiment group; **(C)** Pathologic score statistics for each group; **(D)** Statistics of IL1B immunofluorescence values in each group. ^{##}Compared with the normal group, $P < 0.01$; ^{**}Compared with the model group, $P < 0.01$; NS: no significance. $n = 10$ (control group), $n = 14$ (model group), $n = 14$ (SJZ 400 mg/kg group), $n = 14$ (SJZ 800 mg/kg group), $n = 14$ (300 mg/kg mesalazine group), each repetition is an independent experiment.

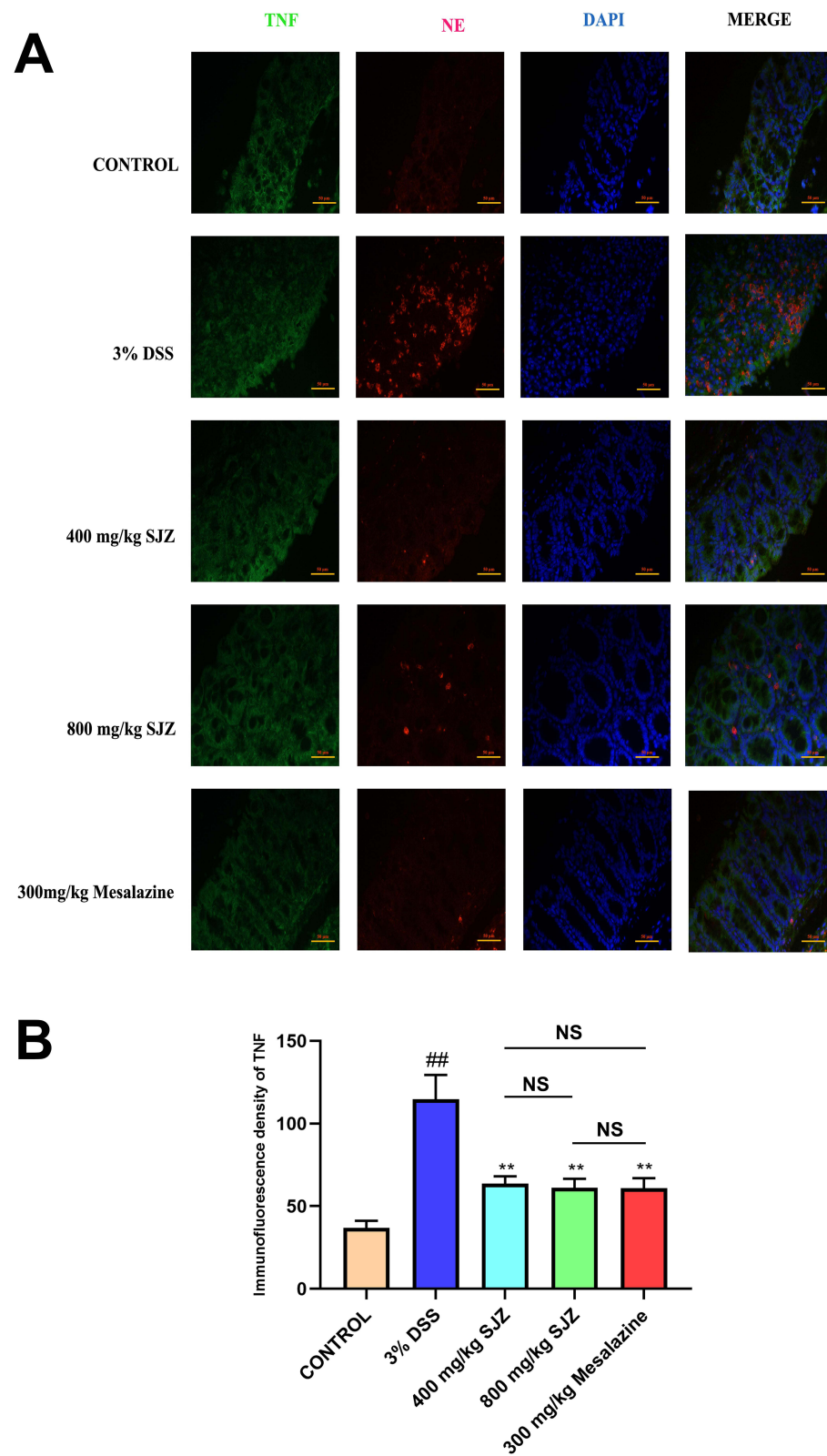


Figure 7 (A and B) Double staining of TNF and NE in colon pathology of mice in each group. ## Compared with the normal group, $P < 0.01$; ** Compared with the model group, $P < 0.01$; NS: no significance. $n = 10$ (control group), $n = 14$ (model group), $n = 14$ (SJZ 400 mg/kg group), $n = 14$ (SJZ 800 mg/kg group), $n = 14$ (300 mg/kg mesalazine group), each repetition is an independent experiment.

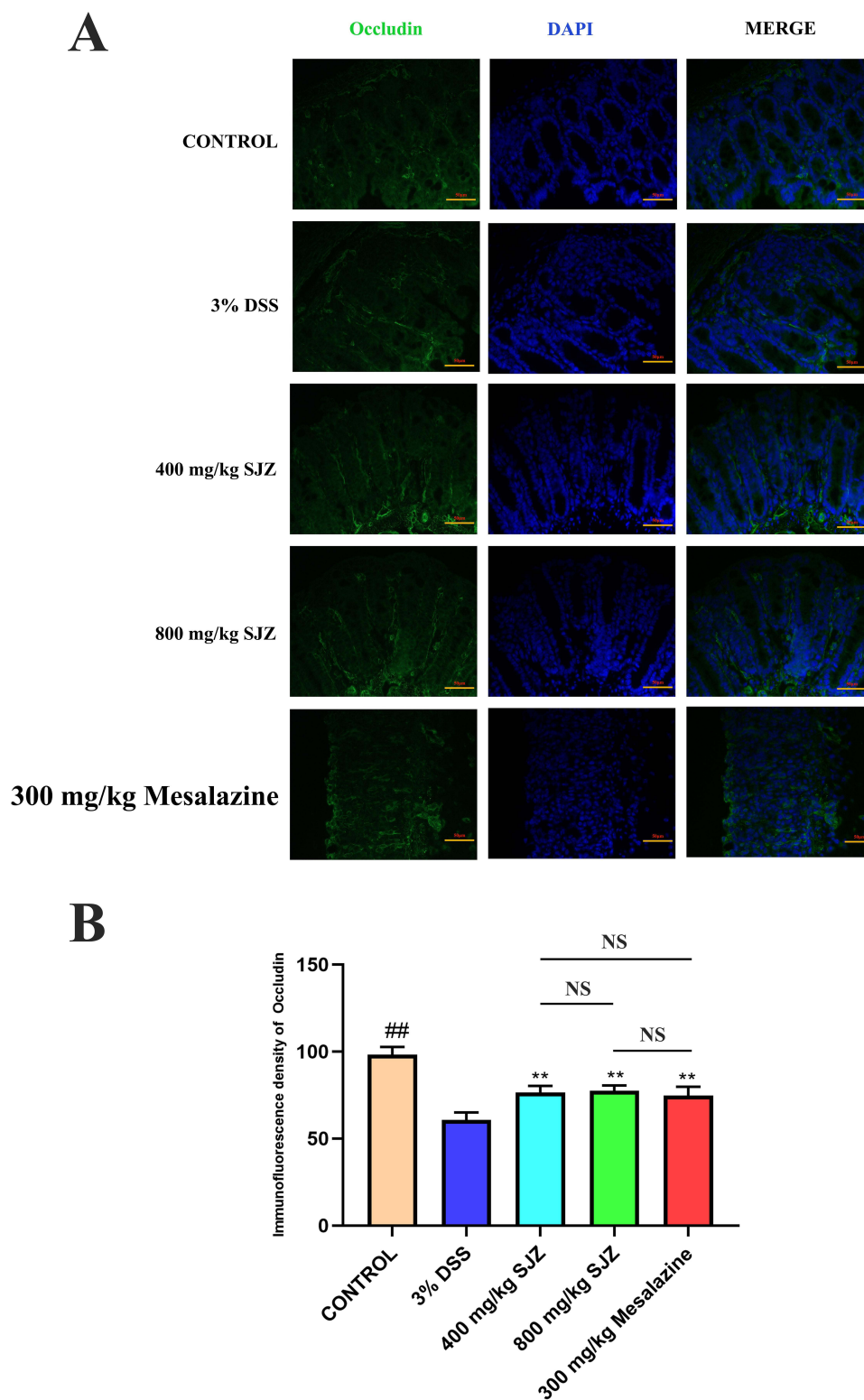


Figure 8 (A and B) Occludin immunofluorescence single staining of colon pathology in each group of mice. ^{##}Compared with the normal group, $P < 0.01$; ^{**}Compared with the model group, $P < 0.01$; NS: no significance. $n = 10$ (control group), $n = 14$ (model group), $n = 14$ (SJZ 400 mg/kg group), $n = 14$ (SJZ 800 mg/kg group), $n = 14$ (300 mg/kg mesalazine group), each repetition is an independent experiment.

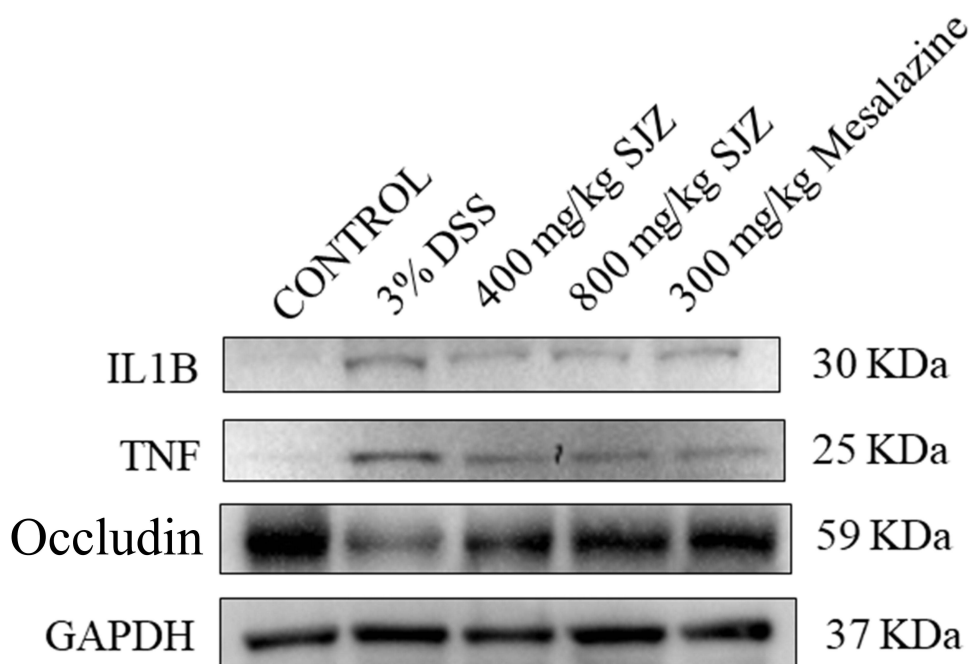


Figure 9 Western blot bands of TNF, IL-1B, and occludin in intestinal mucosa of the mice in each group.

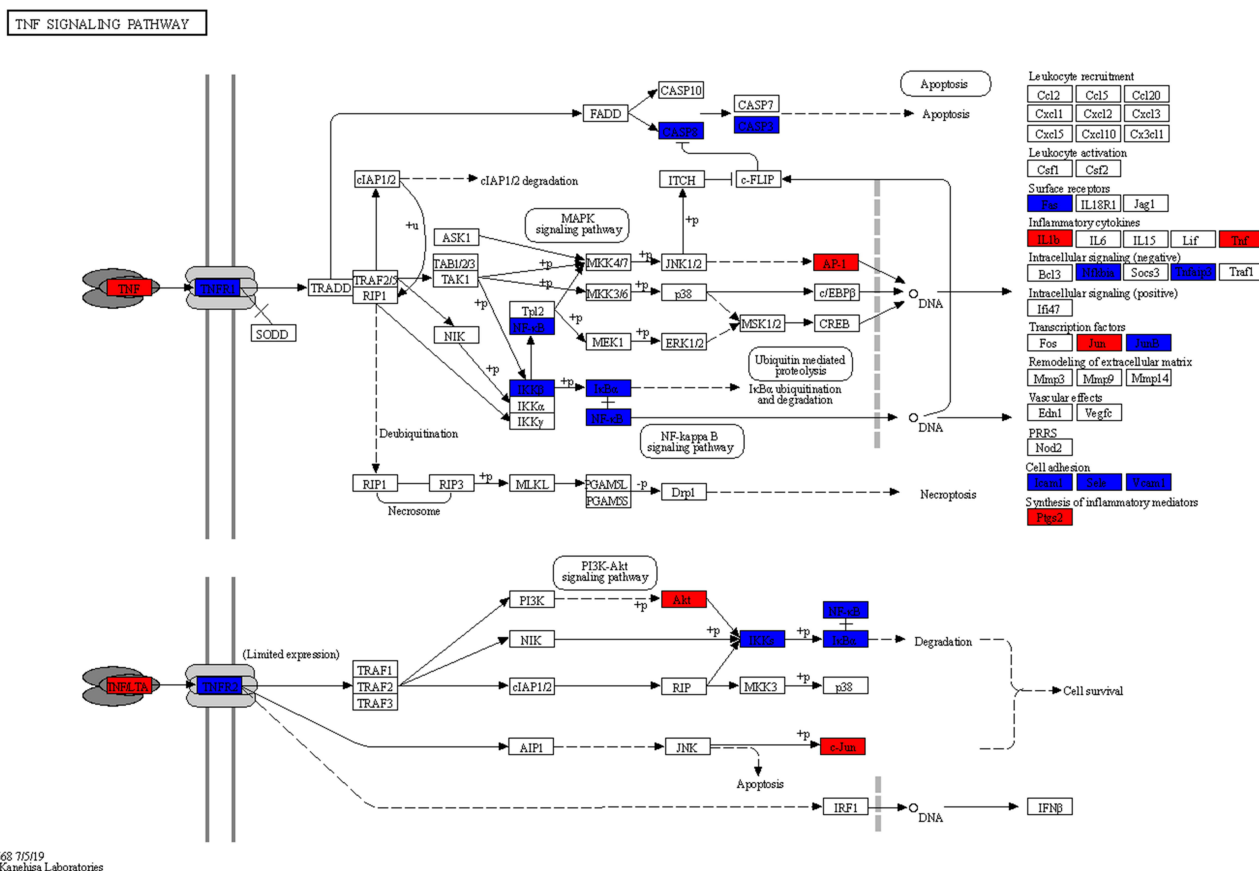


Figure 10 TNF signal diagram. Red indicates important genes for screening SJZ therapy; Blue represents the target of SJZ treatment.

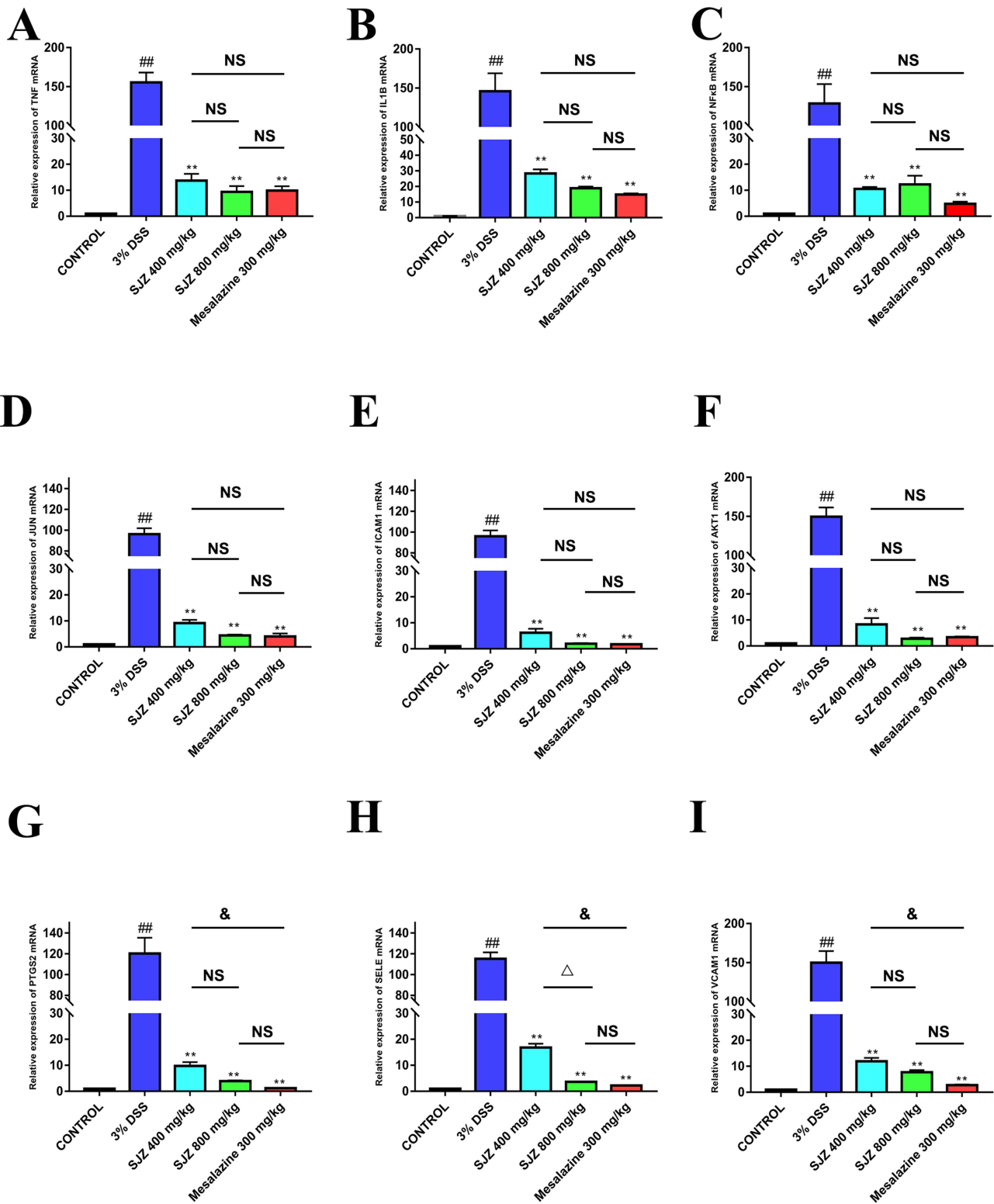


Figure 11 TNF signal results detected by qPCR. (A) The relative expression of IL-1B mRNA in each group; (B) The relative expression of JUN mRNA in each group; (C) The relative expression of TNF mRNA in each group; (D) The relative expression of PTGS2 mRNA in each group; (E) The relative expression of AKT1 mRNA in each group; (F) The relative mRNA expression of (B); (G) The relative mRNA expression of SELE in each group; (H) The relative mRNA expression of ICAM1 in each group; (I) The relative mRNA expression of VCAM1 in each group. NS: no significance. ## Compared to the normal group, $p < 0.01$; ** Compared to the model group, $p < 0.01$; and: Compared to the mesalazine group; Δ : Compared to the SJZ 800 mg/kg group. $n = 3$, each repetition is an independent experiment.

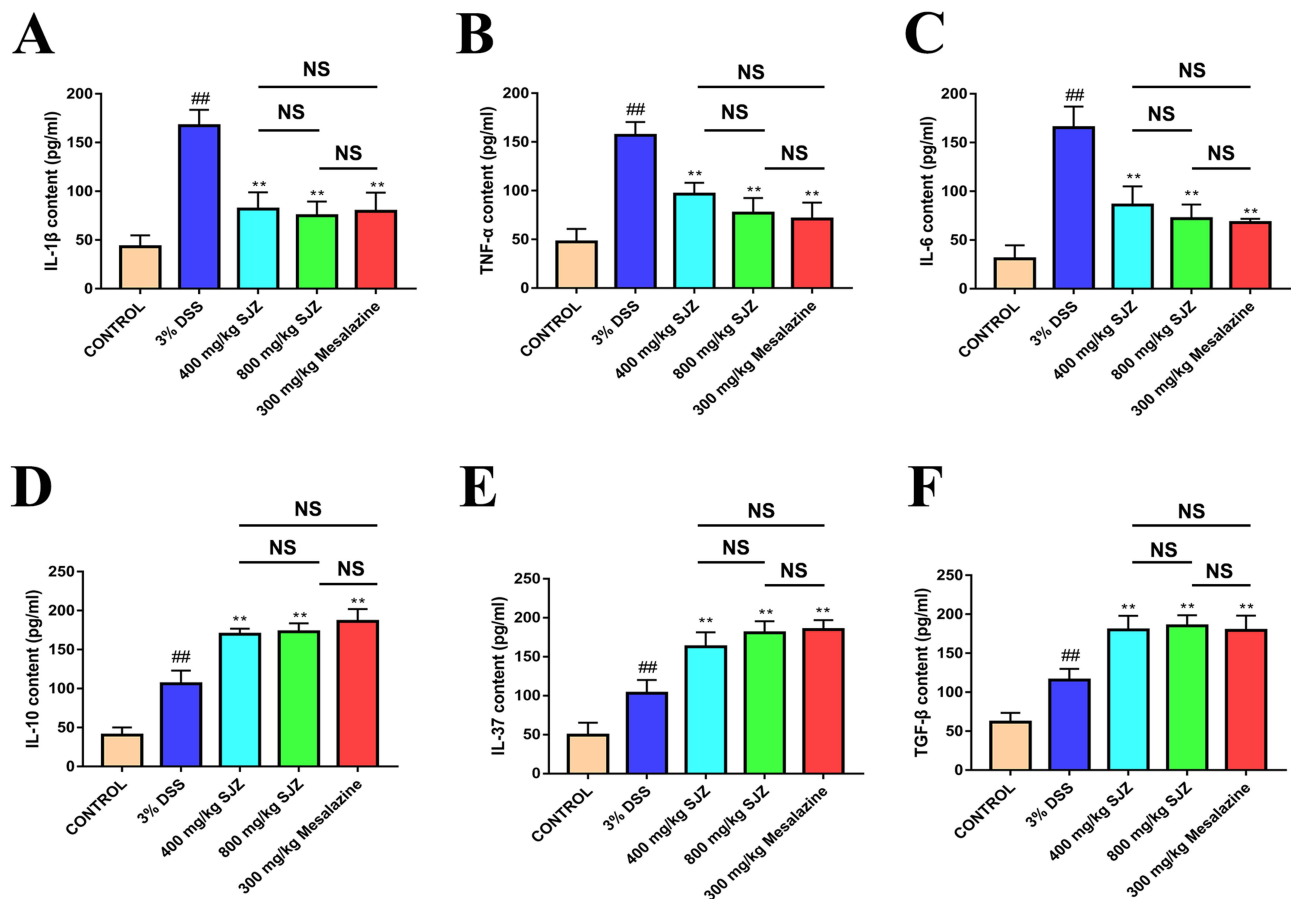


Figure 12 ELISA results of peripheral serum in each group. **(A)** TNF- α content in the serum of each group, content; **(B)** IL-1 β content in the serum of each group; **(C)** IL-6 content in the serum of each group; **(D)** IL-10 content in the serum of each group; **(E)** IL-37 content in the serum of each group; **(F)** TGF- β content content in the serum of each group. ## Compared to the normal group, $p < 0.01$; **Compared to the model group, $p < 0.01$; NS: no significance. $n = 5$, each repetition is an independent experiment.

colitis mice may be to reduce the content of intestinal NETs. The action targets of SJZ in reducing may be IL1B and TNF, and the potential action targets are AKT1, PTGS2 and JUN.

NETs plays an important role in the intestinal immune imbalance of ulcerative colitis⁹. NETs is a double-edged sword for intestinal immunity.¹⁰ NETs can help the intestine to resist harmful external factors, such as bacteria and viruses, in the early stage of ulcerative colitis.⁸ But once the balance between the generation and removal of NETs is broken, excessive NETs will be released into the intestinal mucosa.⁸ NETs contain many proteins and inflammatory factors. With the release of NETs in large quantities, these proteins and inflammatory factors will cause the corresponding inflammatory immune response.⁸ In short, NETs is a trigger of these inflammatory signaling pathways. NETs can be used as a target to curb immune response more quickly, promote intestinal mucosal healing, and reduce the probability of UC replication. Inhibitors developed with NETs targets, such as PADI4 and MPO inhibitors, have been used in clinical trials.^{26,27} In this study, SJZ reduced the levels of NETs, leading to a decrease in the serum levels of pro-inflammatory factors and an increase in anti-inflammatory factors (Figure 12). NETs can also activate numerous inflammatory signaling pathways. Through network pharmacology, we screened TNF as a potential crucial downstream signal of NETs (Figure 2D). In this research, we employed qPCR to validate that SJZ can suppress TNF signaling at the transcriptional level, thereby reducing intestinal inflammation (Figure 11).

In this research, we utilized network pharmacology methods to screen potential targets of SJZ on NETs, with a particular emphasis on the results of molecular docking (Figures 2–4). In the study, we have confirmed that IL1B and TNF are the targets of SJZ on NETs in UC (Figures 6B and 7A). These two proteins are closely related to the development of UC.

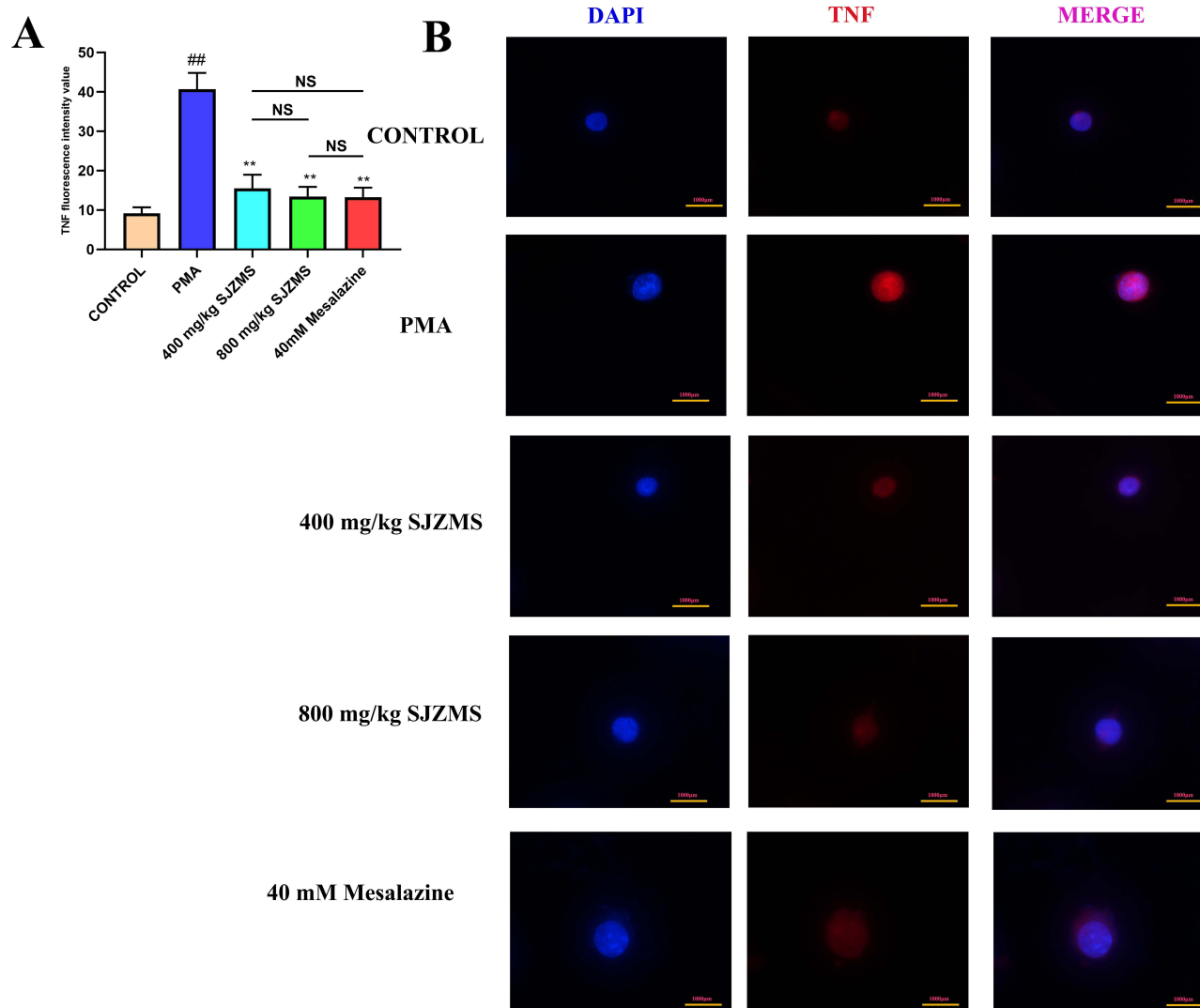


Figure 13 Immunofluorescence detection of TNF in a cellular model of NETs. **(A and B)** compared with the control group, the expression of TNF was higher in the model group, $p < 0.01$; compared with the model group, the expression of TNF was lower in the drug group, $p < 0.01$. ^{##}Compared to the normal group, $p < 0.01$; ^{**}Compared to the model group, $p < 0.01$; NS: no significance. $n = 3$, each repetition is an independent experiment.

IL1B plays a crucial role in intestinal inflammation, closely associated with the function of intestinal epithelial cells, elevated IL1B levels in UC patients, therapeutic effects in colitis model mice, neutrophil activation, intestinal fibrosis, and inflammatory signaling pathways.^{28–33} Additionally, IL1B can also impact intestinal barrier function by modulating MIR200C-3p.³⁴

TNF is involved in various immune-related diseases, particularly in UC, where it affects Treg function and the lifecycle of intestinal epithelial cells.^{35–37} Monoclonal antibody drugs targeting TNF have been developed to rapidly alleviate mucosal inflammation and promote healing in the intestinal mucosa.³⁶

Ginsenoside Rh2 has pharmacological effects such as reducing inflammatory reactions, inhibiting tumor cell proliferation, regulating immunity, reducing the generation of reactive oxygen species, and fighting against aging.³⁸ Reactive oxygen is a critical factor in the generation of NETs.² Given that ROS and inflammation are necessary conditions for producing NETs, we speculate that ginsenoside Rh2 can reduce NETs. Ferromonetin widely exists in traditional Chinese herbs.³⁹ It has a variety of pharmacological effects, including increasing tumor cell death and decreasing tumor cell proliferation, promoting mucosal repair, anti-oxidation, reducing inflammatory reaction, etc.⁴⁰ The mouse model of enteritis can be alleviated by mangiferin.⁴¹ Isoflavone is a joint flavonoid compound. Studies have shown that it

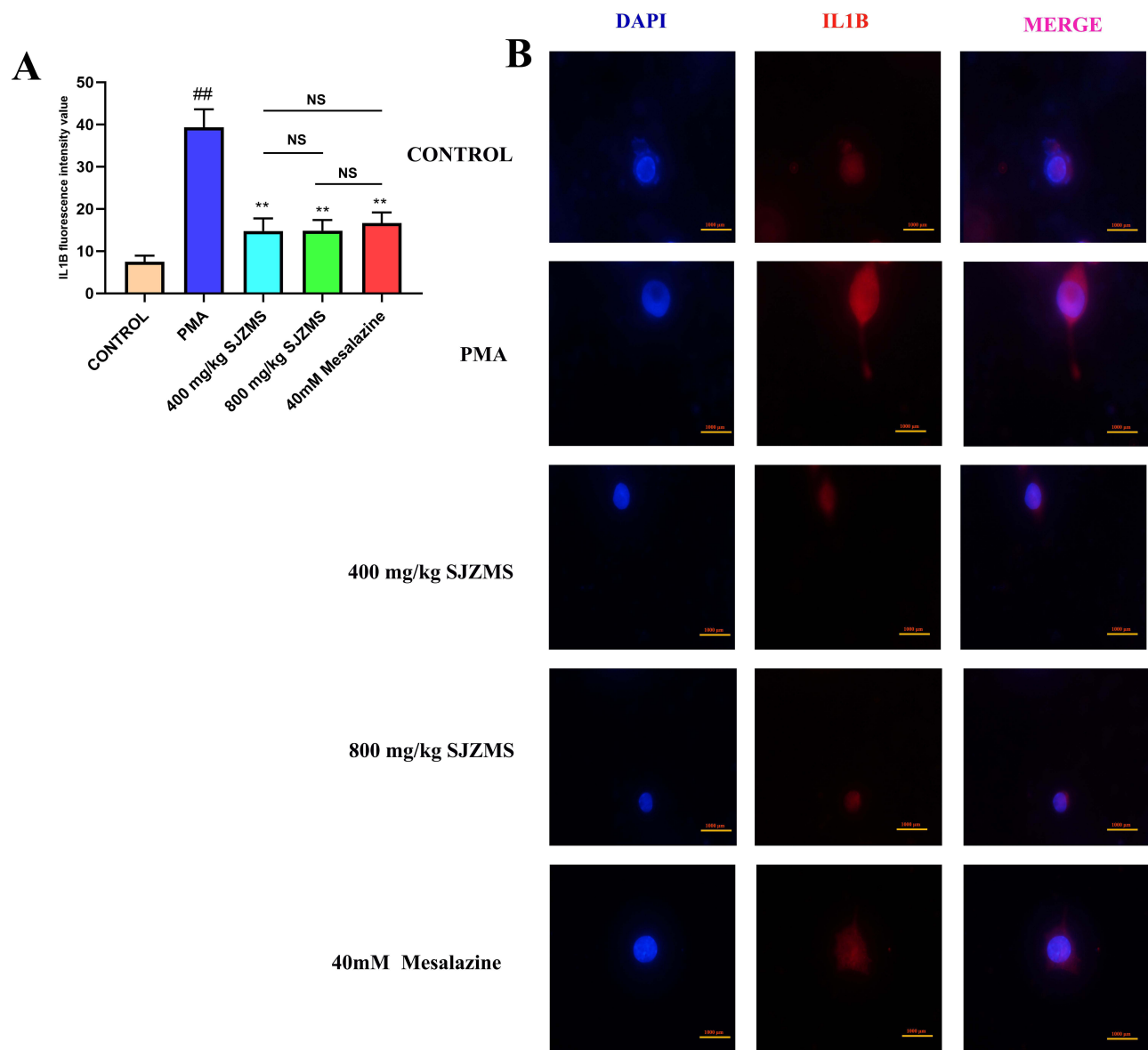


Figure 14 Immunofluorescence detection of IL1B in a cellular model of NETs. (**A** and **B**) compared with the control group, the expression of IL1B was higher in the model group, $p < 0.01$; compared with the model group, the expression of IL1B was lower in the drug group, $p < 0.01$. ^{##}Compared to the normal group, $p < 0.01$; ^{**}Compared to the model group, $p < 0.01$; NS: no significance. $n = 3$, each repetition is an independent experiment.

can reduce intestinal mucosa's inflammatory reaction, increase intestinal mucosa's healing, reduce ROS production, and has a positive regulatory effect on immune cells.⁴² In general, many studies support that ginsenoside Rh2, fermononetin, and isoflavones can regulate immunity, reduce inflammation, and promote intestinal mucosal healing. In the treatment of ulcerative colitis, these drugs have good expected therapeutic effects.

As a famous prescription used for nearly 1000 years in China, Sijunzi Decoction has been used to treat many diseases. In order to ensure the future reproducibility of experiments, we conducted LC-MS analysis on the components contained in this batch of SJZ (Figure 15). At present, a large number of studies have shown that Sijunzi Decoction can improve lipid metabolism, reduce tissue inflammation, regulate human immune function, resist oxidation, and improve the distribution of intestinal flora.⁴³ A meta-analysis showed that Sijunzi decoction was influential in the therapy of UC, which further increased the confidence of Sijunzi decoction in the treatment of UC.¹⁴ There are many mechanisms of Sijunzi decoction in the treatment of ulcerative colitis, but there is no report on the research-oriented to NETs. Therefore, this study screened out the potential targets IL1B, TNF, AKT1, PTGS2, and JUN of Sijunzi Decoction for treating NETs

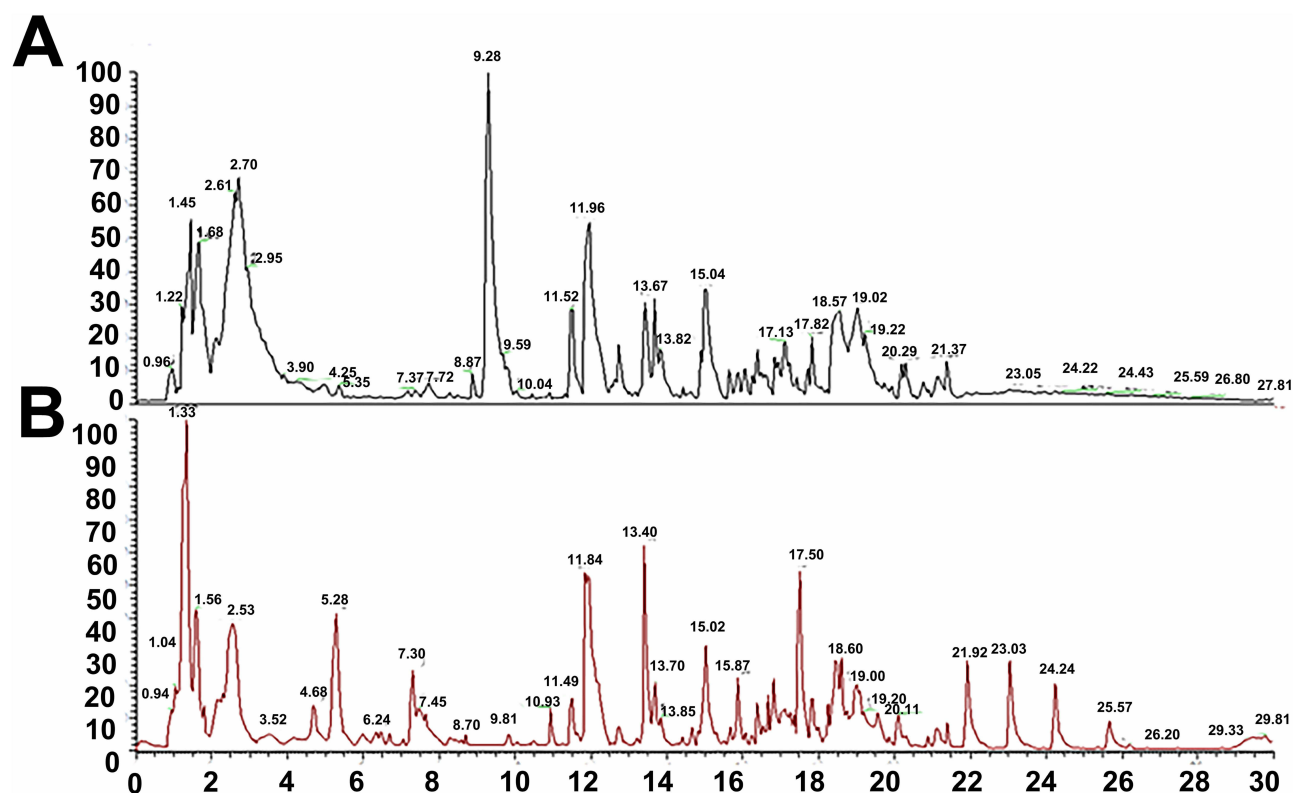


Figure 15 LC-MS of SJZ. (A) Total ion current spectrum of negative ion mode; (B) Total ion current spectrum of positive ion mode.

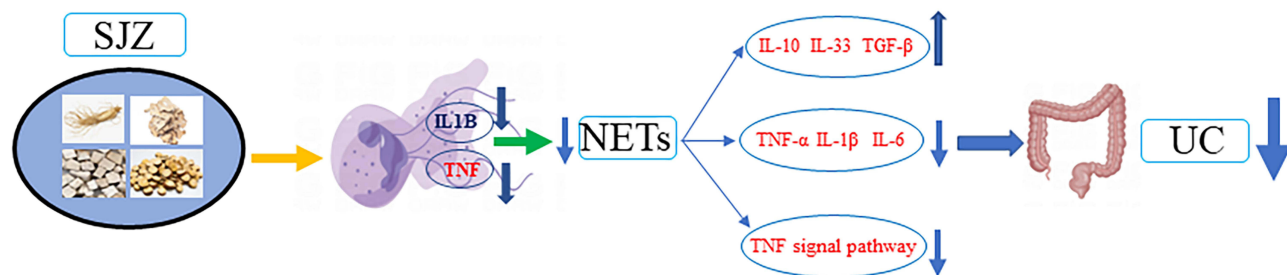


Figure 16 Mechanism diagram of SJZ acting on UC. SJZ reduces the production of NETs through IL1B and TNF. The reduction of NETs can inhibit TNF signals and peripheral serum pro-inflammatory inhibitors, and can promote peripheral serum pro-inflammatory inhibitors, thereby relieving UC.

in UC through the strategy of network pharmacology. And the results of animal experiments confirmed that IL1B and TNF were the explicit targets of Sijunzi Decoction. Ginsenoside Rh2, formononetin, and isoflavones are the possible active components of Sijunzi decoction acting on NETs. This study also has several shortcomings, however. First, although SJZ reduces the production of NETs through IL1B and TNF. The reduction of NETs can inhibit TNF signals and peripheral serum pro-inflammatory inhibitors, and can promote peripheral serum pro-inflammatory inhibitors, thereby relieving UC (Figure 16), the signal mechanism of SJZ decoction on NETs is not specific, and the active ingredients in SJZ decoction have not been tested separately. It is therefore not clear which components of SJZ decoction play the most significant role in reducing intestinal NETs. These are the directions we will focus on in our future endeavors.

Acknowledgments

The authors thank AiMi Academic Services (www.aimieditor.com) for English language editing and review services. National Natural Science Foundation of China (Grant NO:82305105), Guangdong Basic and Applied Basic Research Foundation (Grant NO: 2022A1515110851), Shenzhen Science and Technology Program (Grant NO: JCYJ20220531092005011), the Scientific Research Project of Guangdong Bureau of Traditional Chinese Medicine (Grant NO:20231303) and Sanming Project of Medicine in Shenzhen (No.SZZYSM202211002) support this study. All authors made a significant contribution to the work reported, whether that is in the conception, study design, execution, acquisition of data, analysis and interpretation, or in all these areas; took part in drafting, revising or critically reviewing the article; gave final approval of the version to be published; have agreed on the journal to which the article has been submitted; and agree to be accountable for all aspects of the work.

Disclosure

All the authors in our article do not have any conflicts on economic issues, nor will social relations affect our experimental results.

References

1. Ordás I, Eckmann L, Talamini M, Baumgart DC, Sandborn WJ. Ulcerative colitis. *Lancet*. 2012;380(9853):1606–1619. doi:10.1016/S0140-6736(12)60150-0
2. Eisenstein M. Ulcerative colitis: towards remission. *Nature*. 2018;563(7730):S33. doi:10.1038/d41586-018-07276-2
3. Ungaro R, Mehandru S, Allen PB, Peyrin-Biroulet L, Colombel JF. Ulcerative colitis. *Lancet*. 2017;389(10080):1756–1770. doi:10.1016/S0140-6736(16)32126-2
4. Battat R, Duijvestein M, Guizzetti L, et al. Histologic healing rates of medical therapies for ulcerative colitis: a systematic review and meta-analysis of randomized controlled trials. *Am J Gastroenterol*. 2019;114(5):733–745. doi:10.14309/ajg.000000000000111
5. Feuerstein JD, Moss AC, Farraye FA. Ulcerative Colitis. *Mayo Clin Proc*. 2019;94(7):1357–1373. doi:10.1016/j.mayocp.2019.01.018
6. Dinallo V, Marafini I, Di Fusco D, et al. Neutrophil extracellular traps sustain inflammatory signals in ulcerative colitis. *J Crohns Colitis*. 2019;13(6):772–784. doi:10.1093/ecco-jcc/ijy215
7. Dos Santos Ramos A, Viana GCS, de Macedo Brigido M, Almeida JF. Neutrophil extracellular traps in inflammatory bowel diseases: implications in pathogenesis and therapeutic targets. *Pharmacol Res*. 2021;171:105779. doi:10.1016/j.phrs.2021.105779
8. Drury B, Hardisty G, Gray RD, Ho GT. Neutrophil extracellular traps in inflammatory bowel disease: pathogenic mechanisms and clinical translation. *Cell Mol Gastroenterol Hepatol*. 2021;12(1):321–333. doi:10.1016/j.jcmgh.2021.03.002
9. Abd El Hafez A, Mohamed AS, Shehta A, Sheta H. Neutrophil extracellular traps-associated protein peptidyl arginine deaminase 4 immunohistochemical expression in ulcerative colitis and its association with the prognostic predictors. *Pathol Res Pract*. 2020;216(10):153102. doi:10.1016/j.prp.2020.153102
10. Boeltz S, Amini P, Anders HJ, et al. To NET or not to NET: current opinions and state of the science regarding the formation of neutrophil extracellular traps. *Cell Death Differ*. 2019;26(3):395–408. doi:10.1038/s41418-018-0261-x
11. Bennike TB, Carlsen TG, Ellingsen T, et al. Neutrophil extracellular traps in ulcerative colitis: a proteome analysis of intestinal biopsies. *Inflamm Bowel Dis*. 2015;21(9):2052–2067. doi:10.1097/MIB.0000000000000460
12. Lehmann T, Schallert K, Vilchez-Vargas R, et al. Metaproteomics of fecal samples of crohn's disease and ulcerative colitis. *J Proteomics*. 2019;201:93–103. doi:10.1016/j.jpro.2019.04.009
13. Gottlieb Y, Elhasid R, Berger-Achituv S, Brazowski E, Yerushalmy-Feler A, Cohen S. Neutrophil extracellular traps in pediatric inflammatory bowel disease. *Pathol Int*. 2018;68(9):517–523. doi:10.1111/pin.12715
14. Kou FS, Shi L, Li JX, et al. Clinical evaluation of traditional Chinese medicine on mild active ulcerative colitis: a multi-center, randomized, double-blind, controlled trial. *Medicine*. 2020;99(35):e21903. doi:10.1097/MD.00000000000021903
15. Wei WC, Liaw CC, Tsai KC, et al. Targeting spike protein-induced TLR/NET axis by COVID-19 therapeutic NRICM102 ameliorates pulmonary embolism and fibrosis. *Pharmacol Res*. 2022;184:106424. doi:10.1016/j.phrs.2022.106424
16. Zhou M, Liu Y, Qin H, et al. Xuanfei Baidu decoction regulates NETs formation via CXCL2/CXCR2 signaling pathway that is involved in acute lung injury. *Biomed Pharmacother*. 2023;161:114530. doi:10.1016/j.biopha.2023.114530
17. Chen YM, Deng JM, Wen Y, et al. Modified Sijunzi decoction in the treatment of ulcerative colitis in the remission phase: study protocol for a series of N-of-1 double-blind, randomised controlled trials. *Trials*. 2020;21(1):396. doi:10.1186/s13063-020-04315-0
18. Yu W, Lu B, Zhang H, Zhang Y, Yan J. Effects of the Sijunzi decoction on the immunological function in rats with dextran sulfate-induced ulcerative colitis. *Biomed Rep*. 2016;5(1):83–86. doi:10.3892/br.2016.678
19. Meng-Long Z, Xiao-Yan H, Ya-Lu C, et al. Mechanism and experimental verification of Sijunzi Decoction in treatment of ulcerative colitis based on network pharmacology. *Zhongguo Zhong Yao Za Zhi*. 2020;45(22):5362–5372. doi:10.19540/j.cnki.cjmm.20200810.405
20. Cooper HS, Murthy SN, Shah RS, Sedergran DJ. Clinicopathologic study of dextran sulfate sodium experimental murine colitis. *Lab Invest*. 1993;69(2):238–249.
21. Qu Y, Li X, Xu F, et al. Kaempferol alleviates murine experimental colitis by restoring gut microbiota and inhibiting the LPS-TLR4-NF- κ B Axis. *Front Immunol*. 2021;12:679897. doi:10.3389/fimmu.2021.679897
22. Schwab M, Reynders V, Loitsch S, et al. PPARgamma is involved in mesalazine-mediated induction of apoptosis and inhibition of cell growth in colon cancer cells. *Carcinogenesis*. 2008;29(7):1407–1414. doi:10.1093/carcin/bgn118

23. Stolfi C, De Simone V, Pallone F, Monteleone G. Mechanisms of action of non-steroidal anti-inflammatory drugs (NSAIDs) and mesalazine in the chemoprevention of colorectal cancer. *Int J Mol Sci.* 2013;14(9):17972–17985. doi:10.3390/ijms140917972
24. Zhang R, Zhu X, Bai H, Ning K. Network pharmacology databases for traditional Chinese medicine: review and assessment. *Front Pharmacol.* 2019;10:123. doi:10.3389/fphar.2019.00123
25. Liu Y, Li BG, Su YH, et al. Potential activity of traditional Chinese medicine against ulcerative colitis: a review. *J Ethnopharmacol.* 2022;289:115084. doi:10.1016/j.jep.2022.115084
26. Li H, Fan C, Feng C, et al. Inhibition of phosphodiesterase-4 attenuates murine ulcerative colitis through interference with mucosal immunity. *Br J Pharmacol.* 2019;176(13):2209–2226. doi:10.1111/bph.14667
27. Ahmad G, Chami B, Liu Y, et al. The synthetic myeloperoxidase inhibitor AZD3241 ameliorates dextran sodium sulfate stimulated experimental colitis. *Front Pharmacol.* 2020;11:556020. doi:10.3389/fphar.2020.556020
28. Mitsialis V, Wall S, Liu P, et al. Single-cell analyses of colon and blood reveal distinct immune cell signatures of ulcerative colitis and crohn's disease. *Gastroenterology.* 2020;159(2):591–608.e10. doi:10.1053/j.gastro.2020.04.074
29. Zhang B, Chen H, Ouyang J, et al. SQSTM1-dependent autophagic degradation of PKM2 inhibits the production of mature IL1B/IL-1 β and contributes to LIPUS-mediated anti-inflammatory effect. *Autophagy.* 2020;16(7):1262–1278. doi:10.1080/15548627.2019.1664705
30. Bulek K, Zhao J, Liao Y, et al. Epithelial-derived gasdermin D mediates nonlytic IL-1 β release during experimental colitis. *J Clin Invest.* 2020;130(8):4218–4234. doi:10.1172/JCI1138103
31. Lippai R, Veres-Székely A, Sziksz E, et al. Immunomodulatory role of Parkinson's disease 7 in inflammatory bowel disease. *Sci Rep.* 2021;11(1):14582. doi:10.1038/s41598-021-93671-1
32. Sendler M, van den Brandt C, Glaubitz J, et al. NLRP3 inflammasome regulates development of systemic inflammatory response and compensatory anti-inflammatory response syndromes in mice with acute pancreatitis. *Gastroenterology.* 2020;158(1):253–269.e14. doi:10.1053/j.gastro.2019.09.040
33. Rangaraju S, Dammer EB, Raza SA, et al. Identification and therapeutic modulation of a pro-inflammatory subset of disease-associated-microglia in Alzheimer's disease. *Mol Neurodegener.* 2018;13(1):24. doi:10.1186/s13024-018-0254-8
34. Rawat M, Nighot M, Al-Sadi R, et al. IL1B increases intestinal tight junction permeability by up-regulation of MIR200C-3p, which degrades occludin mRNA. *Gastroenterology.* 2020;159(4):1375–1389. doi:10.1053/j.gastro.2020.06.038
35. Wang D, Huang S, Yuan X, et al. The regulation of the Treg/Th17 balance by mesenchymal stem cells in human systemic lupus erythematosus. *Cell Mol Immunol.* 2017;14(5):423–431. doi:10.1038/cmi.2015.89
36. Panés J, Colombel JF, D'Haens GR, et al. Higher vs standard adalimumab induction and maintenance dosing regimens for treatment of ulcerative colitis: SERENE UC trial results. *Gastroenterology.* 2022;162(7):1891–1910. doi:10.1053/j.gastro.2022.02.033
37. Kalliolias GD, Ivashkiv LB. TNF biology, pathogenic mechanisms and emerging therapeutic strategies. *Nat Rev Rheumatol.* 2016;12(1):49–62. doi:10.1038/nrrheum.2015.169
38. Li X, Chu S, Lin M, et al. Anticancer property of ginsenoside Rh2 from ginseng. *Eur J Med Chem.* 2020;203:112627. doi:10.1016/j.ejmech.2020.112627
39. Machado Dutra J, Espitia PJP, Andrade Batista R. Formononetin: biological effects and uses - A review. *Food Chem.* 2021;359:129975. doi:10.1016/j.foodchem.2021.129975
40. Ong SKL, Shanmugam MK, Fan L, et al. Focus on formononetin: anticancer potential and molecular targets. *Cancers.* 2019;11(5). doi:10.3390/cancers11050611
41. Wu D, Wu K, Zhu Q, et al. Formononetin administration ameliorates dextran sulfate sodium-induced acute colitis by inhibiting NLRP3 inflammasome signaling pathway. *Mediators Inflamm.* 2018;2018:3048532. doi:10.1155/2018/3048532
42. Zhao TT, Jin F, Li JG, et al. Dietary isoflavones or isoflavone-rich food intake and breast cancer risk: a meta-analysis of prospective cohort studies. *Clin Nutr.* 2019;38(1):136–145. doi:10.1016/j.clnu.2017.12.006
43. Guan Z, Wang M, Cai Y, Yang H, Zhao M, Zhao C. Rapid characterization of the chemical constituents of Sijunzi decoction by UHPLC coupled with Fourier transform ion cyclotron resonance mass spectrometry. *J Chromatogr B Analyt Technol Biomed Life Sci.* 2018;1086:11–22. doi:10.1016/j.jchromb.2018.04.009

Drug Design, Development and Therapy

Dovepress

Publish your work in this journal

Drug Design, Development and Therapy is an international, peer-reviewed open-access journal that spans the spectrum of drug design and development through to clinical applications. Clinical outcomes, patient safety, and programs for the development and effective, safe, and sustained use of medicines are a feature of the journal, which has also been accepted for indexing on PubMed Central. The manuscript management system is completely online and includes a very quick and fair peer-review system, which is all easy to use. Visit <http://www.dovepress.com/testimonials.php> to read real quotes from published authors.

Submit your manuscript here: <https://www.dovepress.com/drug-design-development-and-therapy-journal>